

Article

Not peer-reviewed version

Research on Anti-Gastric Cancer Activity of *Panax japonicus* var. *major* and Related Main Functional Compounds

Chao Huang , Ge Li , [Xiuxiang Yan](#) , [Terd Disayathanoowat](#) , [Angkhana Inta](#) , [Lu Gao](#) ^{*} , [Lixin Yang](#) ^{*}

Posted Date: 24 April 2025

doi: 10.20944/preprints202504.2097.v1

Keywords: *Panax japonicus* var. *major*; multiple pathways and targets; metabolite profiling; gastric cancer activities; function mechanisms



Preprints.org is a free multidisciplinary platform providing preprint service that is dedicated to making early versions of research outputs permanently available and citable. Preprints posted at Preprints.org appear in Web of Science, Crossref, Google Scholar, Scilit, Europe PMC.

Copyright: This open access article is published under a Creative Commons CC BY 4.0 license, which permit the free download, distribution, and reuse, provided that the author and preprint are cited in any reuse.

Article

Research on Anti-Gastric Cancer Activity of *Panax japonicus* var. *Major* and Related Main Functional Compounds

Chao Huang ^{1,2,†}, Ge li ^{1,2,†}, Xiuxiang Yan ^{2,3,†}, Terd Disayathanoowat ^{3,4}, Angkhana Inta ³,
Lu Gao ^{1,*} and Lixin Yang ^{1,2,5,*}

¹ School of Ethnic Medicine, Yunnan Minzu University, Kunming 650504, Yunnan, China

² Key Laboratory of Economic Plants and Biotechnology, Kunming Institute of Botany, Chinese Academy of Sciences, Kunming 650201, Yunnan, China

³ Department of Biology, Faculty of Science, Chiang Mai University, 239 Huay Kaew Road, Chiang Mai 50200, Thailand

⁴ Research Center of Deep Technology in Beekeeping and Bee Products for Sustainable Development Goals (SMART BEE SDGs), Chiang Mai University, 239 Huay Kaew Road, Chiang Mai 50200, Thailand

⁵ Southeast Asia Biodiversity Research Institute, Chinese Academy of Sciences, Yezin, Nay Pyi Taw, 05282.

* Correspondence: gl990@foxmail.com (L.G.), rattan@mail.kib.ac.cn (L.Y.)

† Chao Huang, Ge Li and Xiuxiang Yan have contributed equally to this research.

Abstract: Background/Objectives: Gastric cancer is a common malignant tumor worldwide, and few natural substances are available for its effective treatment. The ginseng *Panax japonicus* var. *major* is a natural medicinal plant with anticancer properties in terms of traditional knowledge of indigenous peoples in Yunnan of SW China. **Methods:** In this study, we employed network pharmacology, molecular docking, untargeted metabolomics and molecular dynamics simulations to predict the mode of action of active compounds from *P. japonicus* var. *major* in the treatment of gastric cancer. In vitro experiments and Western blot validation were conducted to validate these predictions. **Results:** Screened 44 main compounds which chikusetsu saponin IVa and calenduloside E inhibit the growth of gastric cancer cells) from *P. japonicus* var. *major* and explored 29 core disease targets which include four core targets (CASP3, TNF, AKT1, EGFR) of gastric cancer through two (TNF and T-cell receptor) signaling pathways. It is important that we not only found that the CASP3 and Chikusetsu saponin IVa formed a structurally stable complex with strong binding via multiple hydrogen bonds, but also revealed that both exert anti-gastric cancer effects by downregulating the Bcl-2/Bax ratio and upregulating the expression of CASP3 and CASP9 proteins, and provided the significant difference in anti-gastric cancer activity between two extracts from fresh and dried *P. japonicus* var. *major*. **Conclusion:** This results may provide a scientific supporting for indigenous medicine usage of *P. japonicus* var. *major* for gastric cancer treating and need further Pharmacological experiments and clinical experiments.

Keywords: *Panax japonicus* var. *major*; multiple pathways and targets; metabolite profiling; gastric cancer activities; function mechanisms

Introduction

Gastric cancer (GC) is a major type of malignant tumor and a leading cause of death worldwide, ranking fifth in terms of incidence and mortality rates. Furthermore, the incidence of GC among young people is on the rise [1]. GC patients who cannot be treated by surgery have no other treatment options, and the survival rate of patients with advanced GC is only 20% in the past way [2]. Therefore, it is urgently necessary to find drugs that can treat GC or be used as adjuvant therapy.

Non-targeted metabolomics approach was used to investigate the anticancer and immunomodulatory effects of fermented *Perilla frutescens* leaves. [3]. A combination of network pharmacology and molecular docking experiments was used to clarify the active ingredients from the fungus *Armillaria ostoyae* that contribute to GC treatment and the related pathways they may target [4]. Molecular docking and clinical medical research can be combined to help predict the mechanism of drug-activated diseases and improve the therapeutic efficacy of drug-activated lesions [5].

The biological pathways and regulatory genes targeted by bioactive compounds from medicinal plants have recently been studied for the treatment of GC. Several medicinal plants possess noted anti-GC properties, for example *Paris polyphylla* [6]; *Radix Astragali*, the root of *Astragalus membranaceus* var. *mongholicus* [7]; *Pseudostellaria heterophylla* (Miq.) Pax [8]; and *Curcuma longa* L [9]. Previous studies showed that natural antitumor drugs with clinical applications mainly are alkaloids [10], terpenoids [11], polyphenols [12], and polysaccharides [13]; most of these compounds display high efficacy in treating GC. For instance, treatment with taxol, which interferes with the microtubules of GC cells, blocks mitotic progression and interrupts cell growth, thus inducing the shrinkage of GC cells and eventually apoptosis [14]. Alkaloids can activate crosstalk between apoptosis and autophagy by inhibiting the phosphoinositide 3-kinase (PI3K)/Akt/mammalian target of rapamycin (mTOR) pathway and thus repress the viability of GC cells [15]. Moreover, an alkaloid derived from the marine fungus *Arthrinium arundinis* inhibited the growth and metastasis of GC cells by targeting the mTORC1 signaling pathway [16]. Although much progress has been made in the study of natural antitumor compounds, few (taxol being one) have significant antitumor efficacy. Therefore, more research is needed to explore natural antitumor compounds through the integration of biological pathways and genes affected by these chemicals.

Panax japonicus var. *major* is a species of ginseng that is mainly distributed in the Yunnan province of China [17] and belongs to the genus *Panax*, from the Araliaceae family. From the roots of this traditional Chinese medicinal plant, 122 compounds were isolated and identified, mainly consisting of saponins and flavonoids [18]. Total saponins from *P. japonicus* var. *major* have been reported to possess anticancer, immunomodulatory, anti-inflammatory, analgesic, cardioprotective, hepatoprotective, and antioxidant activities [19–23]. Extracts from *P. japonicus* var. *major* have been used for the treatment of inflammation, hepatocellular carcinoma, ischemic brain damage, and other diseases [24]. However, there has been little research on the possible treatment of GC with this medicinal plant.

Investigating the effects of this medicinal plant on GC and their mechanisms requires researchers to identify the main active compounds in *P. japonicus* var. *major* extracts and their cellular targets. Therefore, the purpose of this study was to assess the therapeutic efficacy and mechanism of action of *P. japonicus* var. *major* extracts for the treatment of GC. This study provides a theoretical basis for the deployment of natural medicinal herbs for GC treatment.

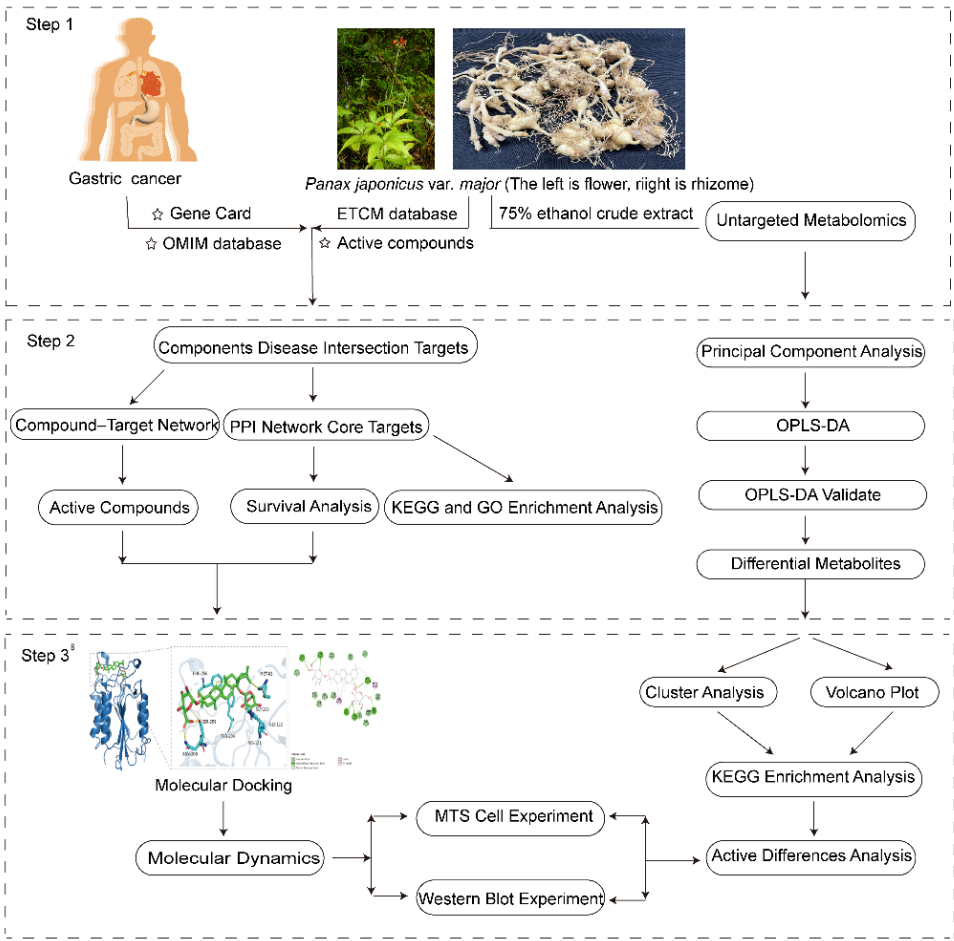


Figure 1. Analysis workflow of network and untargeted metabolomics.

2. Results

2.1. Screening for Active Ingredients and Gastric Cancer Targets

To this end, we first obtained a list of 44 known *P. japonicus* var. *major* active compounds from the ETCM database (Figure S1). These active compounds were mainly saponins with anticancer and anti-inflammatory activities, including Chikusetsu saponin IVa; the ginsenosides Ro, Rc, and Re; taibaienoside I; panaxjapyne A; panaxjapyne B; and panaxjapyne C, [25,26]. We then predicted the cellular targets of these 44 compounds using the Swiss Target Prediction tool, which identified 355 potential targets of active compounds. Separately, we assembled a list of 2,103 GC targets by screening the Gene Cards and OMIM databases with the keyword “gastric cancer”. Comparison of the 355 predicted targets for active compounds from *P. japonicus* var. *major* and the 2,103 GC targets defined a set of 125 common targets.

2.2. Main Components and Targets Associated with Gastric Cancer

To examine how these 125 predicted common targets interact, we constructed a component–target map and the underlying protein–protein interaction (PPI) network (Figure 2A). We screened each main active ingredient and their corresponding targets and ranked them according to their degree, betweenness, and closeness values. We chose the top ten active compounds for analysis (Table 1): panaxjapyne C, panaxjapyne B, cholesterol,β-Sitosterol, stigmasterol, notoginsenoside-R2, 3,4,5-trimethoxybenzoic acid, Chikusetsu saponin IVa, stipuleanoside R2, and calenduloside E.

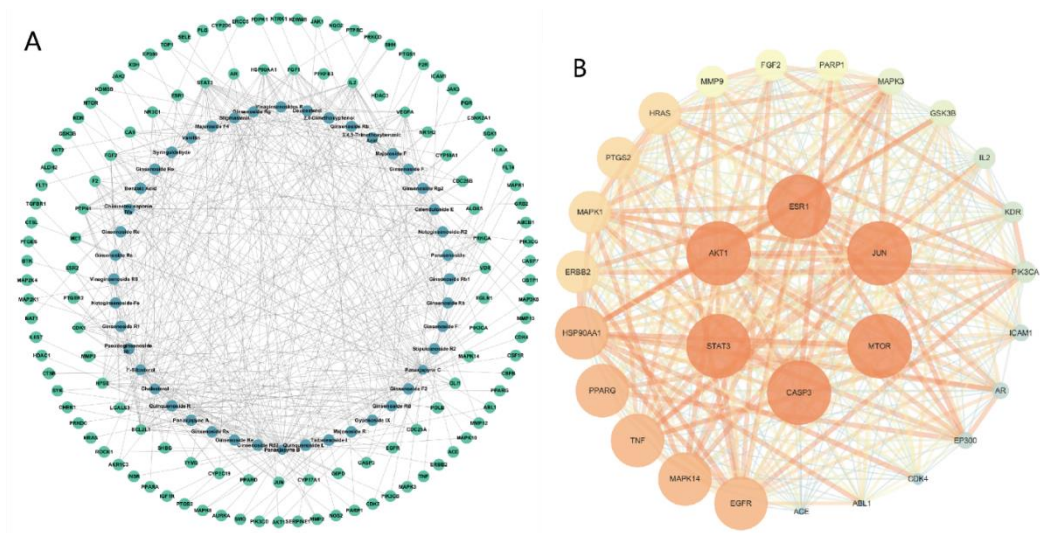
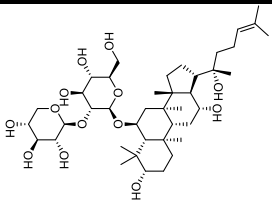
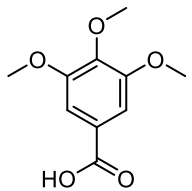
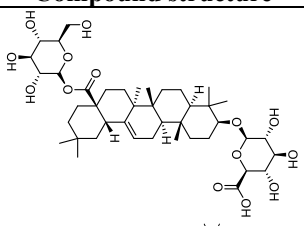
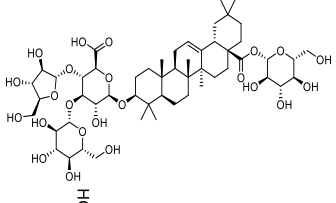
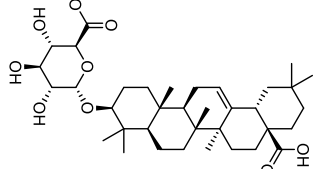


Figure 2. Identification of key active ingredients and core disease targets through network pharmacology. (A) Compound–target network. Blue nodes represent active compounds and green nodes represent targets. (B) Protein–protein interaction network.

Separately, we drew the PPI network of all 125 common targets and their interactors based on data obtained from the STRING database in Cytoscape3.10.2 (Figure 2B).The visualization of the PPI network used the following settings: closeness > 0.046, betweenness > 99.70, degree > 33.07. The top 29 targets for treatment of GC, based on decreasing degree values, are listed in Table 2; these targets are potentially associated with GC.

Table 1. The top 10 active compounds based on decreasing degree values from *P. japonicus* var. *major*.

Compound name	Compound structure	Degree	Betweenness	Closeness
Panaxjapyne C		45.0	8,980.48	0.23108666
Panaxjapyne B		45.0	8,888.03	0.22919509
Cholesterol		22.0	2,596.21	0.20512821
β-Sitosterol		19.0	1,565.01	0.20363636
Stigmasterol		17.0	1,001.37	0.20071685

Notoginsenoside R2		13.0	759.52	0.19421965
3,4,5TrimethoxybenzoicAcid		12.0	3,169.00	0.19156215
ChikusetsusaponinIVa		12.0	1,601.09	0.20664206
Stipuleanoside R2		11.0	739.68	0.20023838
Calenduloside E		11.0	782.38	0.20715167

Note: Degree, betweenness, and closeness values are based on the network shown in Figure 1A.

Table 2. The top 29 gastric cancer targets ranked by their degree value in the PPI network.

Protein name	Degree	Protein name	Degree
AKT1	96	MAPK14	61
TNF	93	GSK3B	59
EGFR	87	MAPK1	59
CASP3	84	KDR	58
STAT3	84	EP300	58
JUN	83	HRAS	58
ESR1	78	FGF2	56
HSP90AA1	74	PARP1	54
ERBB2	73	IL2	53
MMP9	73	ICAM1	48
MAPK3	69	CDK4	47
MTOR	69	ABL1	46
PTGS2	67	AR	44
PPARG	67	ACE	34
PIK3CA	62		

Note: Degree values are based on the network shown in Figure 1B.

2.3. Potential Functions and Pathways Associated with Targets for GC Treatment

We explored the potential mechanisms and pathways enriched among the common targets by conducting gene ontology (GO) term and Kyoto Encyclopedia of Genes and Genomes (KEGG) pathway enrichment analysis of the 29 core targets. We identified 313 terms related to biological processes (BP), 34 terms related to cellular component (CC), 54 terms related to molecular function (MF), and 141 KEGG pathways as being enriched; the top 10 terms or pathways are shown as bubble diagrams in (Figure 3). The predicted effects of compounds derived from *P. japonicus* var. *major* were mainly related to 'negative regulation of gene expression' and 'positive regulation of protein phosphorylation' (Figure 3A) among the top 10 BP terms. The common targets mostly localized to the cytoplasm and the nucleus (Figure 3B). The MF terms enriched in common targets (Figure 3C) were 'identical protein binding', 'enzyme binding', and 'ATP binding'.

The top 20 enriched KEGG pathways are shown in (Figure 3D). Three KEGG pathways highly enriched in common targets were associated with apoptosis, including the tumor necrosis factor (TNF) signaling pathway, the T-cell receptor signaling pathway, and the interleukin 17 (IL-17) signaling pathway, which are also closely associated with triggering inflammation. We also constructed a component-pathway-target diagram (Figure 4) by combining the top 20 KEGG pathways, 29 core GC targets, and 44 main active compounds. We determined that these 44 chemical compounds are associated with the core targets caspase 3 (CASP3), TNF, and AKT1, which function primarily in the TNF and p53 signaling pathways in the treatment of GC.

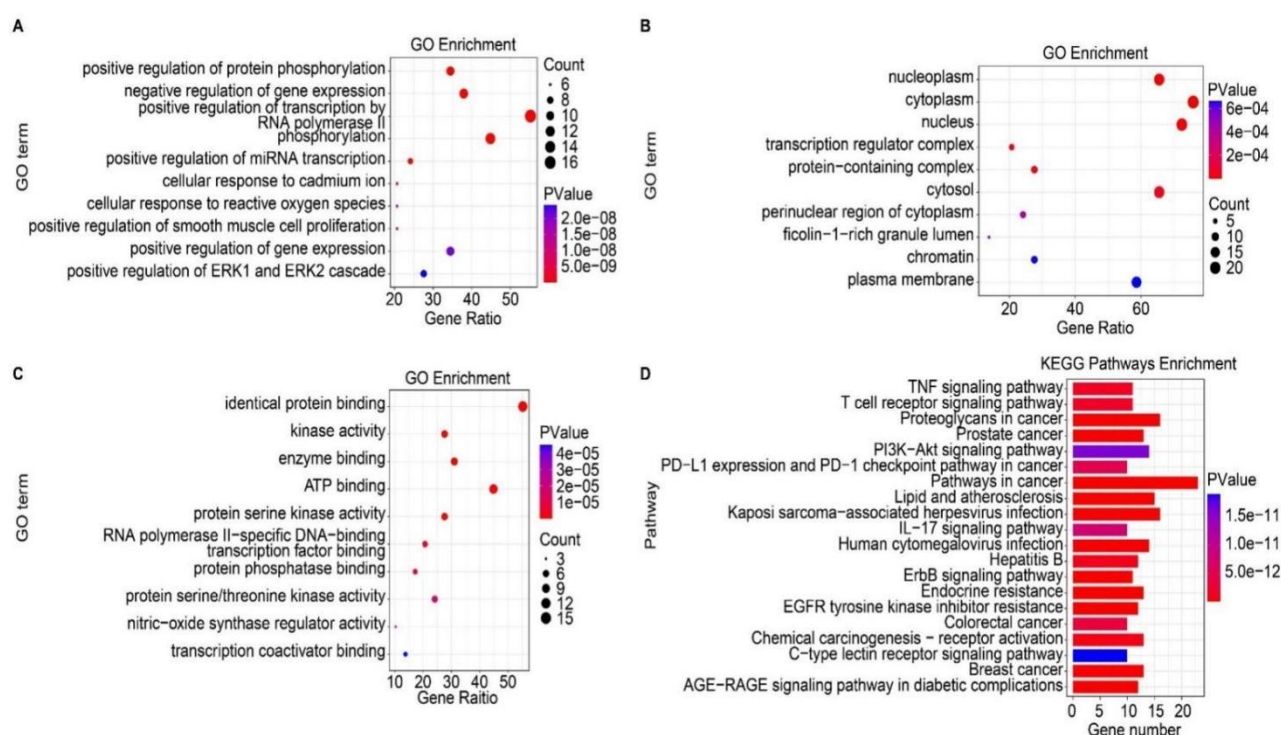


Figure 3. KEGG and GO enrichment analysis of all 29 core targets. (A–C) GO term enrichment for biological processes (A), cellular components (B), and molecular function (C). (D) KEGG pathway enrichment analysis.

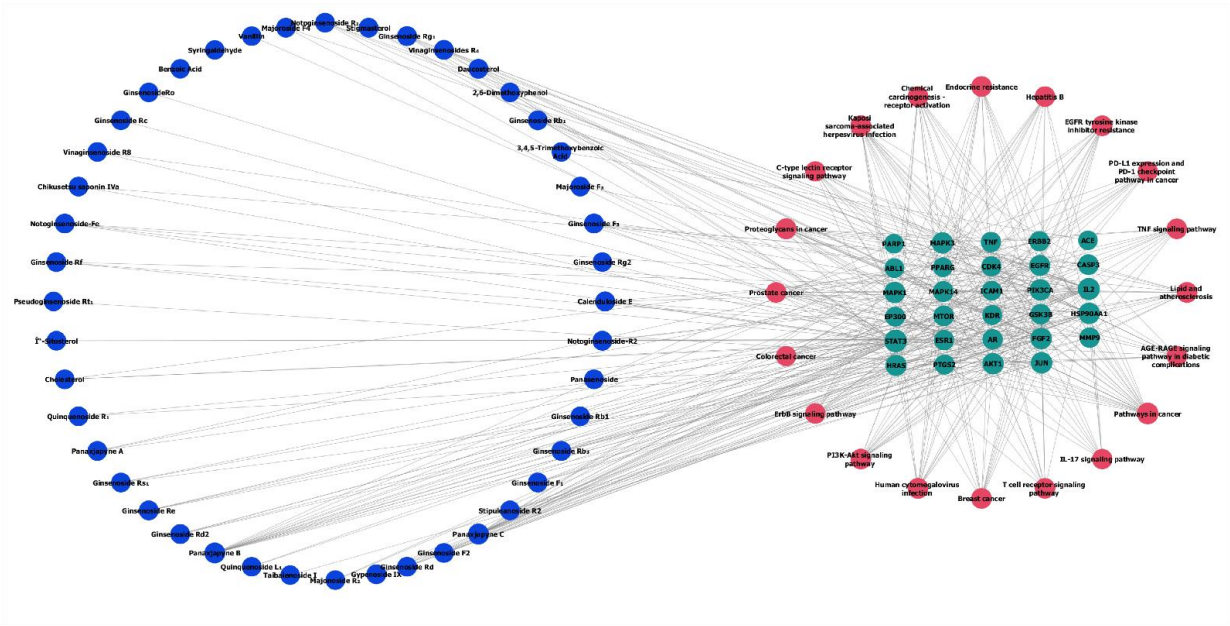
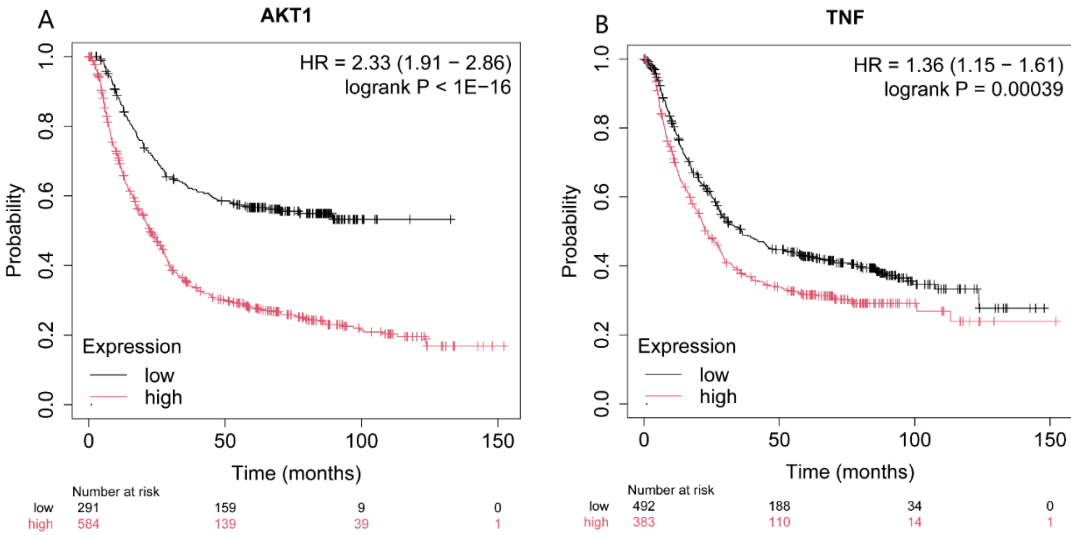


Figure 4. Component–pathway–target network of *P. japonicus* var. *major* active compounds and their potential targets. The blue nodes represent compounds, the red nodes indicate pathways, and the green nodes represent core disease targets.

2.4. Effect on Four Genes Expression Associated with Patients’ Survival Period

We looked for an association between clinical patient survival and the expression of each of the top four core target genes, *CASP3*, *AKT1*, *TNF*, and *EGFR*. Specifically, we generated Kaplan-Meier plots to assess patient survival at $P < 0.05$ (Figure 5). When either *AKT1*, *TNF*, or *EGFR* was expressed at a low level, patient survival was higher than when the gene was expressed at a higher level (Figure 5A–C). By contrast, higher *CASP3* expression was associated with patient survival (Figure 5D).



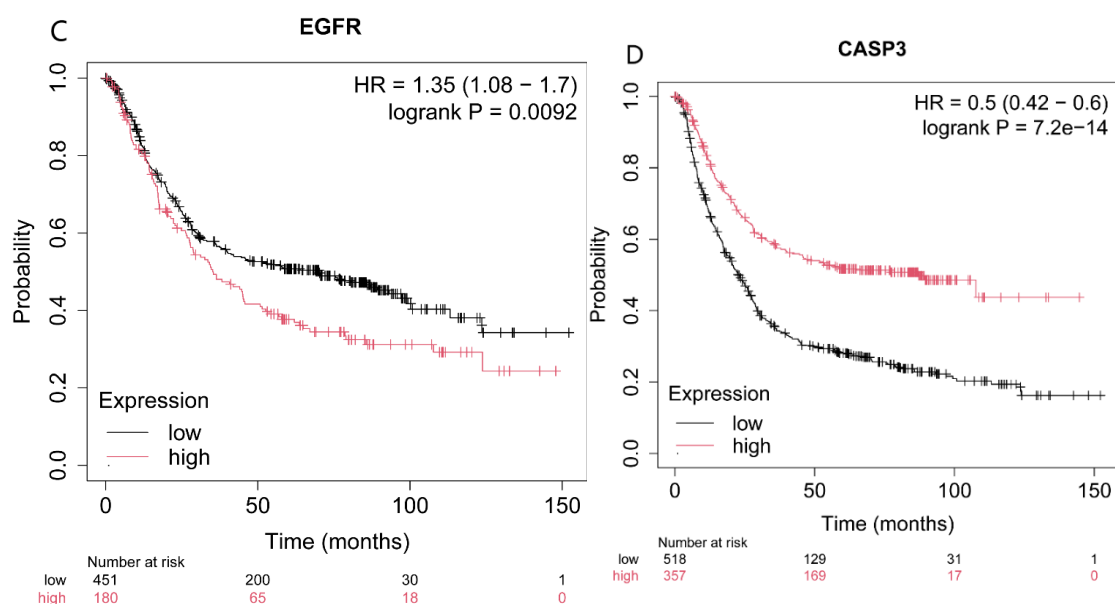
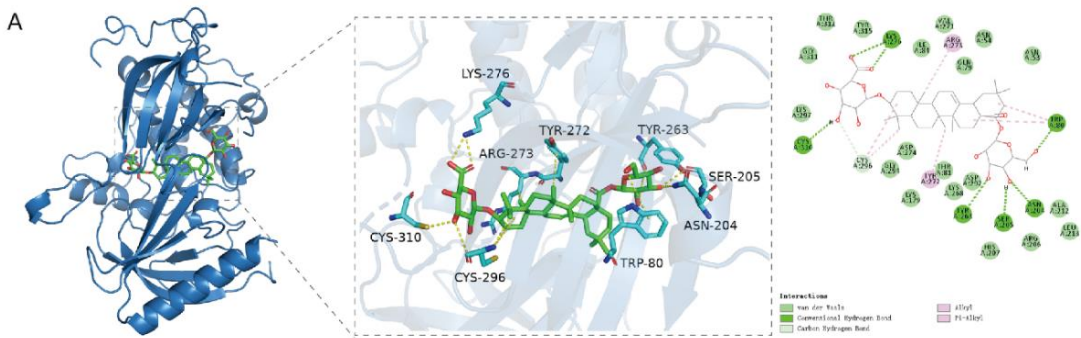


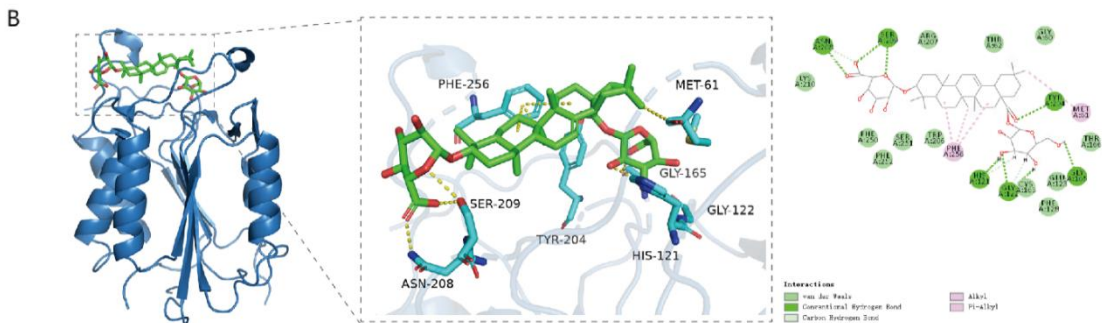
Figure 5. Survival curves for gastric cancer patients as a function of expression levels for four target genes. (A) AKT1. (B) TNF. (C) EGFR. (D) CASP3. The probability of survival following GC diagnosis is shown for patients with low (black curves) or high (red curves) expression for the indicated gene.

2.5. Binding Ability Between Main Active Compounds and Protein Targets

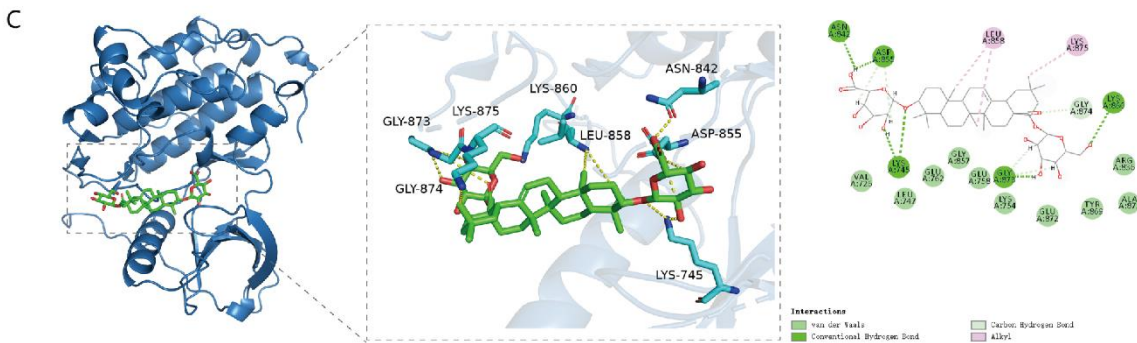
To examine the potential effects of *P. japonicus* var. *major* active compounds (Chikusetsu saponin IVa and Calenduloside E) on the four proteins identified above, we subjected these four target proteins (CASP3, AKT1, TNF, and EGFR) to a molecular docking analysis using MOE2019 software [27]. The molecular docking analysis indicated that Chikusetsu saponin IVa and calenduloside E can access the binding pockets of AKT1, TNF, EGFR, and CASP3, with molecular docking energies ranging from -6.19 to -10.46 kcal/mol for these eight compounds–target pairs. Of these eight pairs, six (Chikusetsu saponin IVa–AKT1, Chikusetsu saponin IVa–CASP3, Chikusetsu saponin IVa–EGFR, calenduloside E–AKT1, calenduloside E–CASP3, and calenduloside E–EGFR) showed strong binding activity, whereas the remaining two pairs (Chikusetsu saponin IVa–TNF, calenduloside E–TNF) had weaker binding activity. The details of molecular docking between the compounds and the targets are shown in Figure 6. For example, residues Lys-276, Cys-310, Trp-80, Ser-205, Asn-204, and Tyr-263 of AKT1 formed hydrogen bonds with Chikusetsu saponin IVa, whereas residues Arg-273, Tyr-272, and Cys-296 formed hydrophobic interactions. Residue Cys-296 of AKT1 formed a hydrocarbon interaction with Chikusetsu saponin IVa (Figure 6A). Asn-208, Ser-209, Tyr-204, His-121, Gly-122, and Gly165 of CASP3 formed hydrogen bonds with Chikusetsu saponin IVa; Phe-256 and Met-261 formed hydrophobic interactions; and the Gly-122 and Asn-208 residues formed hydrocarbon interactions (Figure 6B). Asn-842, Asp-855, Lys-745, Gly-873, and Lys-860 of EGFR formed hydrogen bonds with Chikusetsu saponin IVa (Figure 6C). Asp-273, Lys-204, and Leu-240 of TNF formed hydrogen bonds with Chikusetsu saponin IVa (Figure 6D). Lys-297, Cys-296, Tyr-272, and Val-270 of AKT1 formed hydrophobic interactions with calenduloside E (Figure 6E). Gly-122, Cys-163, Ser-120, Arg-64, and Ser-205 of CASP3 interacted with calenduloside E by forming hydrogen bonds (Figure 6F). Cys-797, Leu-844, Val-726, and Leu-718 of EGFR formed hydrophobic interactions with calenduloside E (Figure 6G). Finally, Asp-145, Thr-143, Glu-189, Lys-283, Lys-252, and Tyr-192 of TNF formed hydrogen bonds with calenduloside E (Figure 6H). Importantly, the docking energy values of all compounds were less than -5.0 kcal/mol, indicating strong binding to each of their targets.



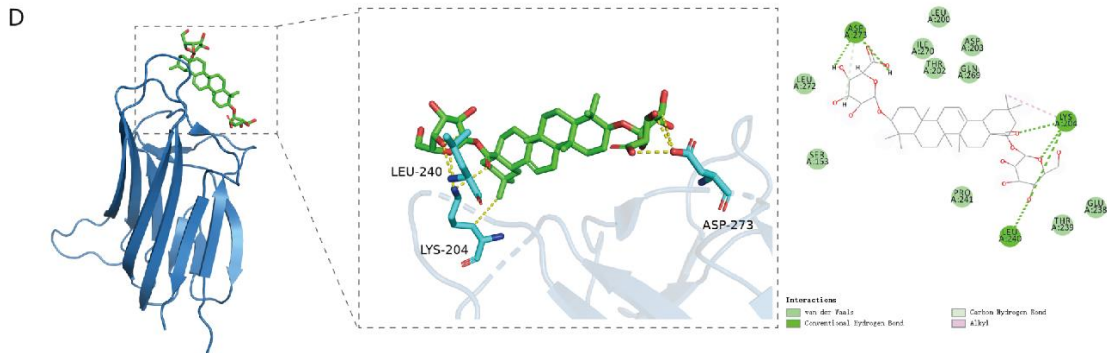
Chikusetsu saponin IVa bound to AKT1 (PDB: 7NH5) BE: -10.46 kcal/mol.



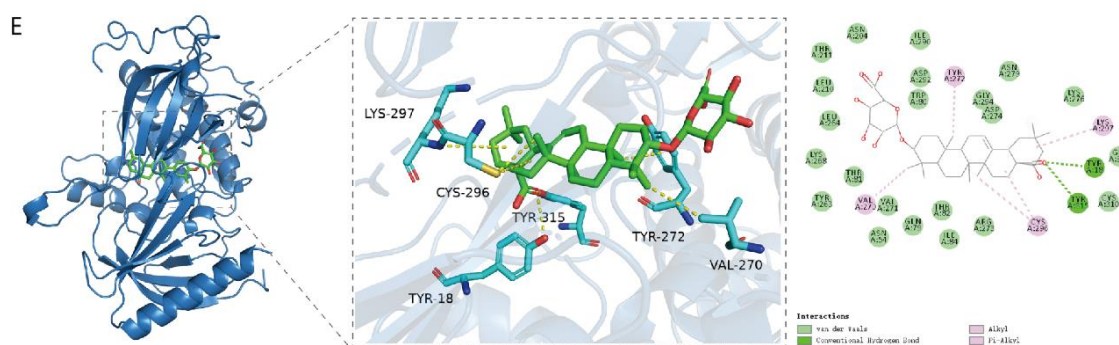
Chikusetsu saponin IVa bound to CASP3 (PDB: 1CP3) BE: -8.20 kcal/mol



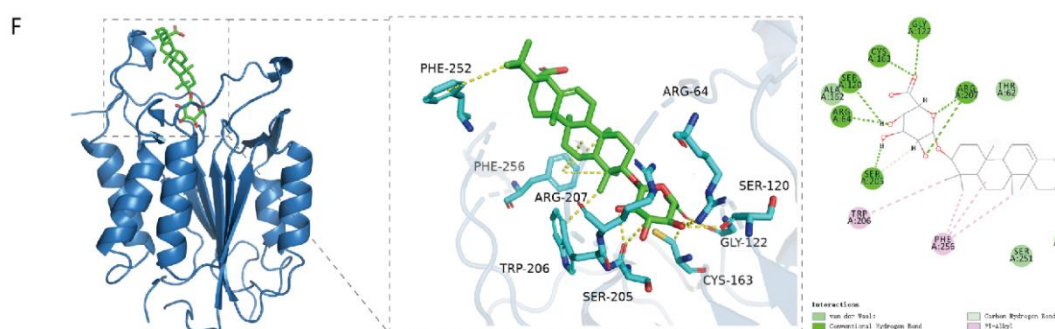
Chikusetsu saponin IVa bound to EGFR (PDB: 5UGB) BE: -8.38 kcal/mol



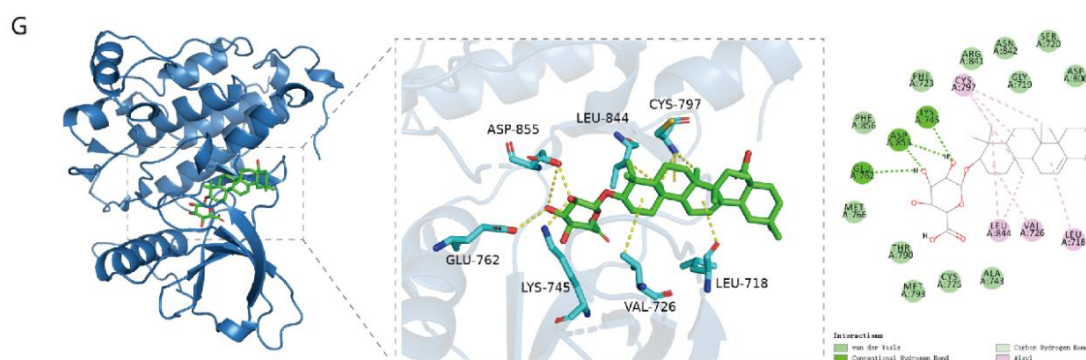
Chikusetsu saponin IVa bound to TNF (PDB: 1KXG) BE: -6.48 kcal/mol



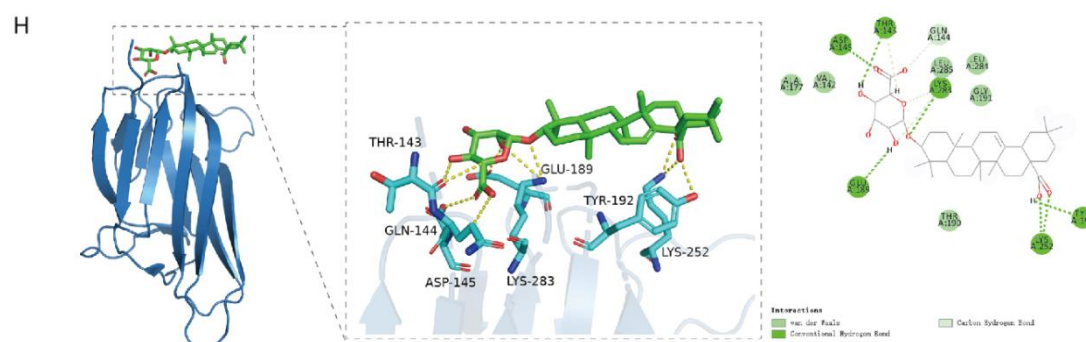
Calendulose E bound to AKT1 (PDB: 7NH5) BE: -8.93 kcal/mol



Calendulose E bound to CASP3 (PDB: 1CP3) BE: -7.45 kcal/mol



Calendulose E bound to EGFR (PDB: 5UGB) BE: -7.48 kcal/mol



Calendulose E bound to TNF (PDB: 1KXG) BE: -6.19 kcal/mol

Figure 6. Molecular docking between the two active compounds Chikusetsu saponin IVa and calendulose E and the four target proteins AKT1, CASP3, EGFR and TNF. (A–H) Prediction of molecular docking of Chikusetsu saponin IVa onto AKT1 (PDB: 7NH5) (A), Chikusetsu saponin IVa onto CASP3 (PDB: 1CP3) (B), Chikusetsu saponin IVa onto EGFR (PDB: 5UGB) (C), Chikusetsu saponin IVa onto TNF (PDB: 1KXG) (D), calendulose E

onto AKT1 (PDB: 7NH5) (E), calenduloside E onto CASP3 (PDB: 1CP3) (F), calenduloside E onto EGFR (PDB: 5UGB) (G), and calenduloside E onto TNF (PDB: 1KXG) (H).

2.6. Binding Energy and Stability of Chikusetsu Saponin IVa–CASP3

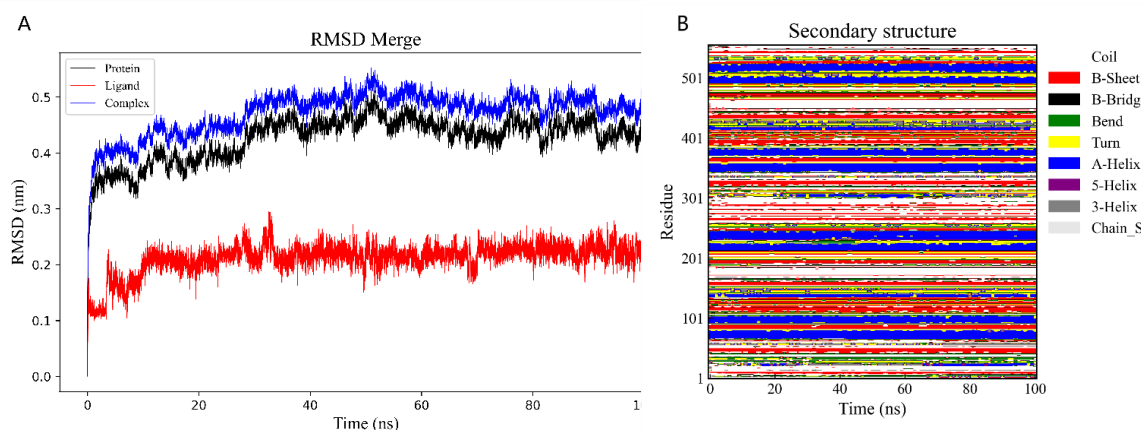
We assessed the interaction strength of Chikusetsu saponin IVa in complex with CASP3 through molecular dynamics simulations. We used RMSD values as indicators of structural changes in CASP3 [28] and Chikusetsu saponin IVa (Figure 7A). This analysis indicated that the first 20 ns of binding between CASP3 and the small molecule involve a large change in RMSD value, with an MD simulation over 100 ns. For RMSD values < 0.5 Å, the CASP3–Chikusetsu saponin IVa complex, Chikusetsu saponin IVa ligand and CASP3 protein showed an average a value of 0.43, 0.21, and 0.45 Å, respectively. These results suggest that CASP3 is structurally stable when bound to Chikusetsu saponin IVa.

To verify the stability of CASP3 secondary structure, we calculated the change in secondary structure by molecular dynamics simulations. The secondary structure of CASP3 remained essentially stable in MD simulations in the first step (Figure 7B). We then calculated RMSF values between CASP3 and Chikusetsu saponin IVa to identify localized fluctuations in CASP3 structure. The RMSF values of the proteins were smaller in the bound portion and larger in the unbound portion, it is shown that the binding of small molecules had some effect on the stability of the protein. (Figure 7C), suggesting that small molecule binding has an effect on protein stability.

In MD simulations, we calculated the Solvent-Accessible Surface Area (SASA) value for carbon (C) in CASP3 to analyze the change in surface area before and after binding of Chikusetsu saponin IVa to CASP3. The SASA value was relatively larger before CASP3 bound to Chikusetsu saponin IVa and then decreased and stabilized after binding (Figure 7D), indicative of a decrease in the surface area of CASP3 concomitant with an increase in the number of H-bonds between CASP3 and Chikusetsu saponin IVa (Figure 7E).

We calculated the binding free energy of CASP3 in complex with Chikusetsu saponin IVa to assess the stability of the complex. Specifically, we calculated the Molecular Mechanics Poisson-Boltzmann Surface Area (MMPBSA) [29]; the results are shown in (Table 3).

Free energy landscape diagrams can clearly reflect interactions and energy distribution between systems [30], and can also help clarify the interactions between small molecules and proteins, along with possible changes in conformation. Thermodynamically more stable conformations usually correspond to regions of lower free energy, whereas less stable conformations correspond to regions of higher free energy. The complex between CASP3 and Chikusetsu saponin IVa had an energy minimum mainly concentrated around 99 ns during the 100-s duration of the MD simulation (Figure 8). The complex was relatively compact in this low-energy region, and the structure appeared to be able to remain stable in this state for some time.



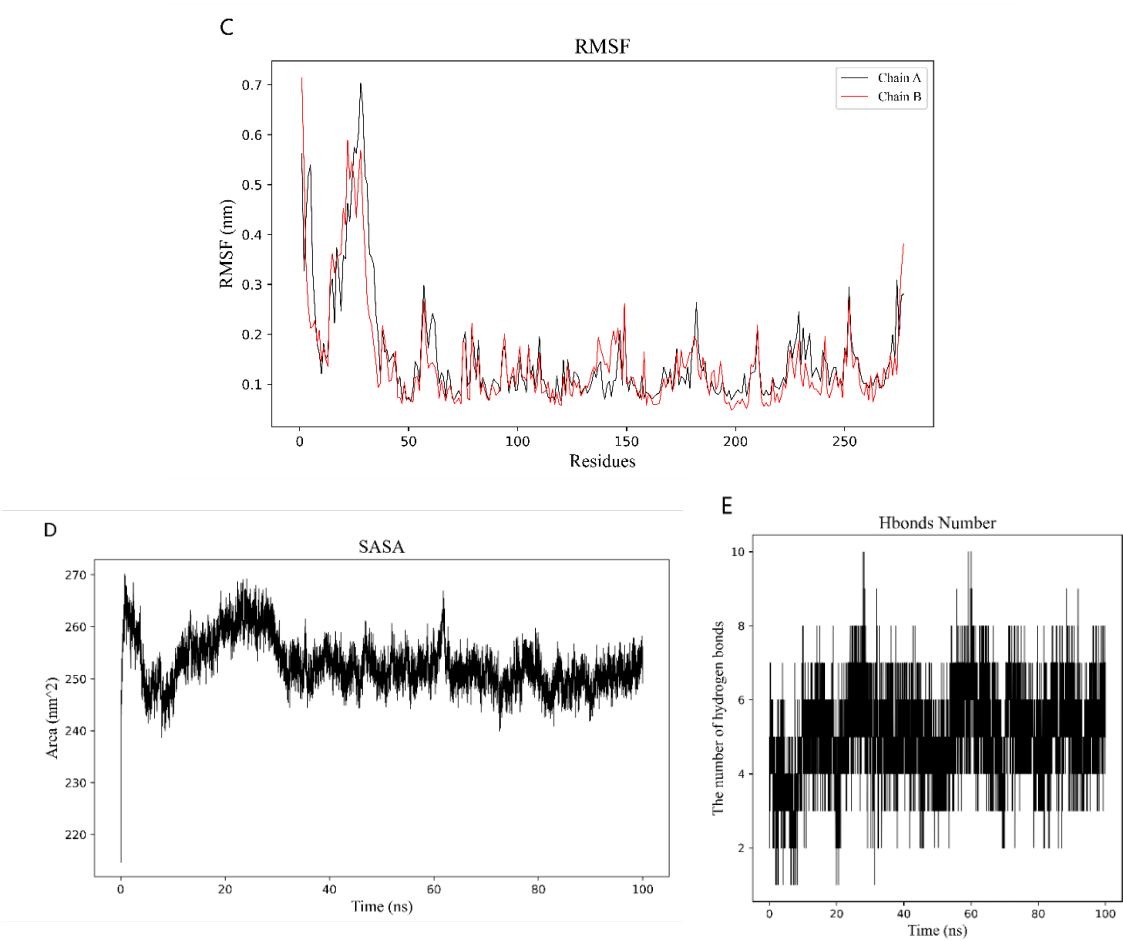


Figure 7. Molecular dynamics simulations. (A) RMSD values as a function of time. (B) Secondary structure. (C) RMSF values along the protein sequence. (D) SASA values of complexes as a function of time. (E) Number of H-bonds.

Table 3. Binding free energies of the indicated complexes.

CASP3–Chikusetsu saponin IVa	
Van der Waals force	-70.74 ± 1.28
EEL	-54.74 ± 1.96
EGB	78.59 ± 4.05
ESURF	-9.88 ± 0.09
ΔG_{GAS}	-125.48 ± 2.34
ΔG_{SOLV}	68.70 ± 4.05
$\Delta Total$	-56.77 ± 4.68

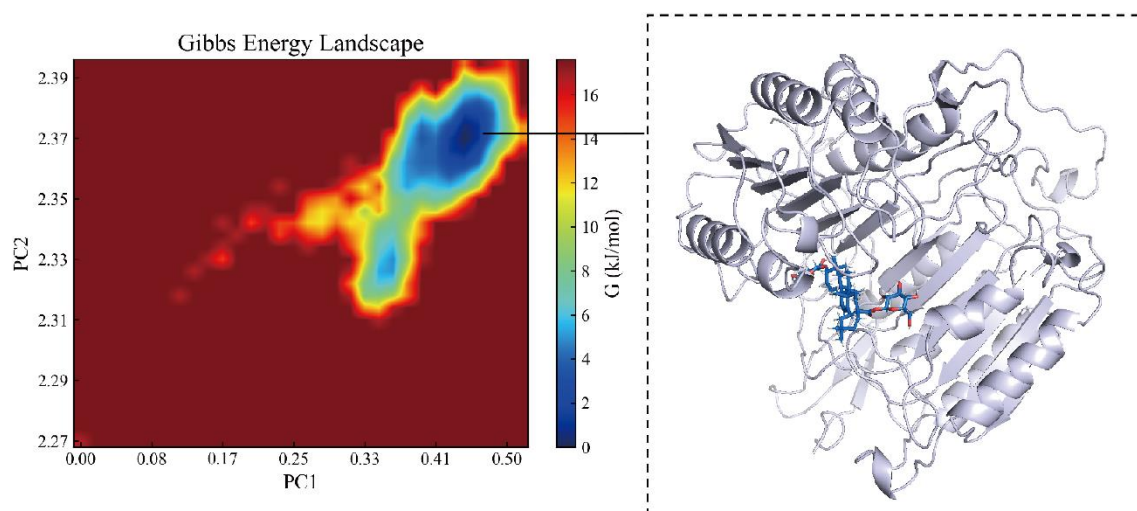


Figure 8. Free energy conformational map.

2.7. Analysis of Major Components and Differential Metabolites in *Panax japonicus*

Principal Component Analysis (PCA) revealed obvious distinction between the dried and fresh *P. japonicus* var. *major* (Figure 9). Dried samples were clustered on the left side of PC1, and the fresh ones on the right, indicating great metabolic distinction. PC1 and PC2 accounted for 69.28% and 19.19% of the total variance, respectively, suggesting a good structured and reliable model. Partial Least Squares Discriminant Analysis (PLS-DA), as shown in Figure 10A, presented a distinct separation between ZZS-G and ZZS-S with tight clustering and good reproducibility. The prediction results were very close to those of PCA, which also indicated the strength of the model. From (Figure 10B), the model yielded a Q^2 of 0.997, indicating very good predictability. Moreover, both Q^2 and R^2Y had p -values smaller than 0.005, attesting to the statistical significance and reliability of the model.

Volcano plot analysis on the differential metabolites of the fresh and dried groups revealed both significant statistical significance and remarkable relative abundance changes. 914 metabolites were significantly upregulated and 1,297 significantly downregulated (Figure 11A). Based on the cluster analysis of the differential metabolites in *P. japonicus* var. *major*, the result indicated that amino acids and derivatives, organic acids, and alkaloids were the key differential metabolites between two groups (Figure 11B).

The KEGG pathway enrichment analysis was performed based on these differential metabolites. As shown in (Figure 12), the most enriched pathways included phenylalanine metabolism, isoquinoline alkaloid biosynthesis, tropane, piperidine and pyridine alkaloid biosynthesis, and arginine biosynthesis. These pathways are presumably related to gastric cancer [31–34], which suggests that the remarkable differences in anti-gastric cancer activity between the fresh and dried *Panax japonicus* var. *major* extracts may be caused by the alterations in the biosynthesis of these metabolites.

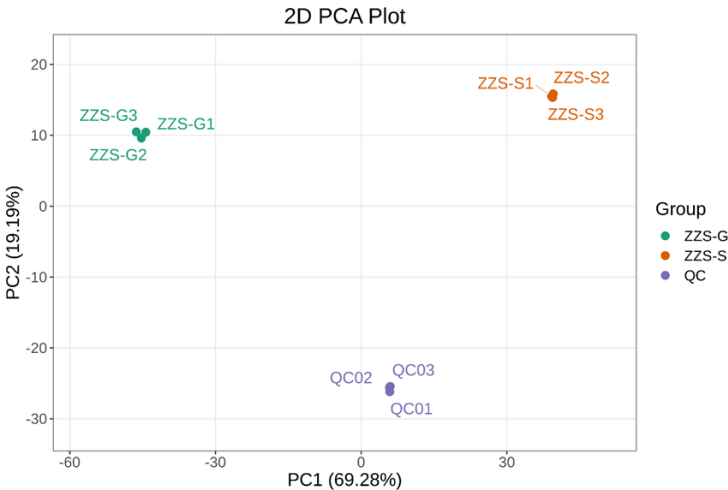


Figure 9. Principal component analysis plot. In the PCA score plot, each point represents one individual sample, and samples from the same group are colored the same. “Group” represents the corresponding experimental grouping. PC1, PC2, and PC3 represent the first, second, and third principal components, respectively, and their corresponding contribution rates represent the percentage of variance in the data explained.

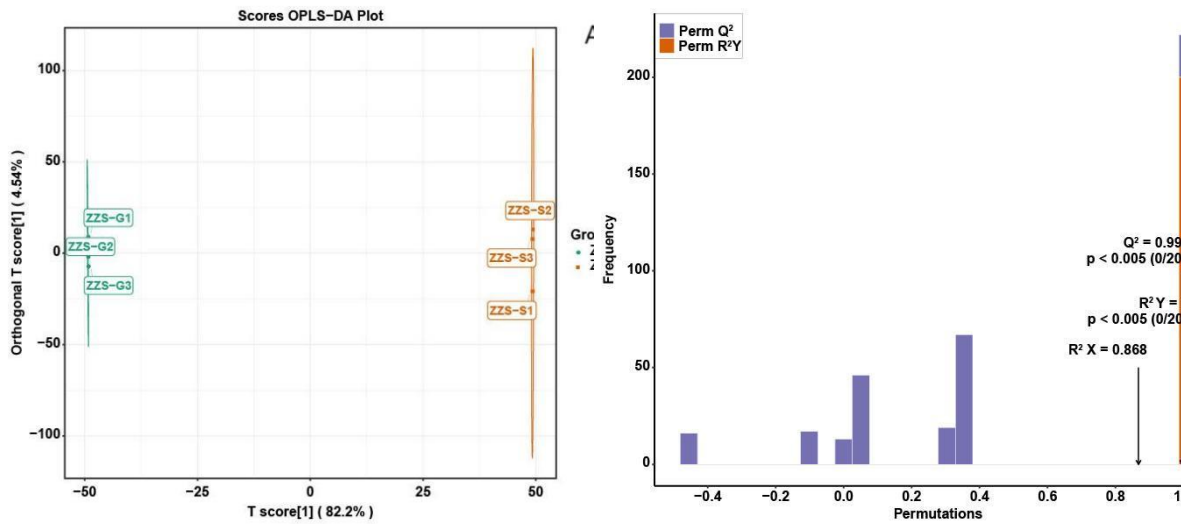


Figure 10. Partial least squares discriminant analysis. (A) In the score plot, each point represents one sample, and samples of the same group are represented by the same colors; “Group” means the corresponding sample category. In the permutation test plot, (B) the x-axis represents the R^2Y and Q^2 values of the model, and the y-axis represents the frequency of classification accuracy across 200 random permutations. Orange and purple bars indicate R^2Y and Q^2 values from the permuted models, respectively, with black arrows indicating the original model’s R^2X , R^2Y , and Q^2 values.

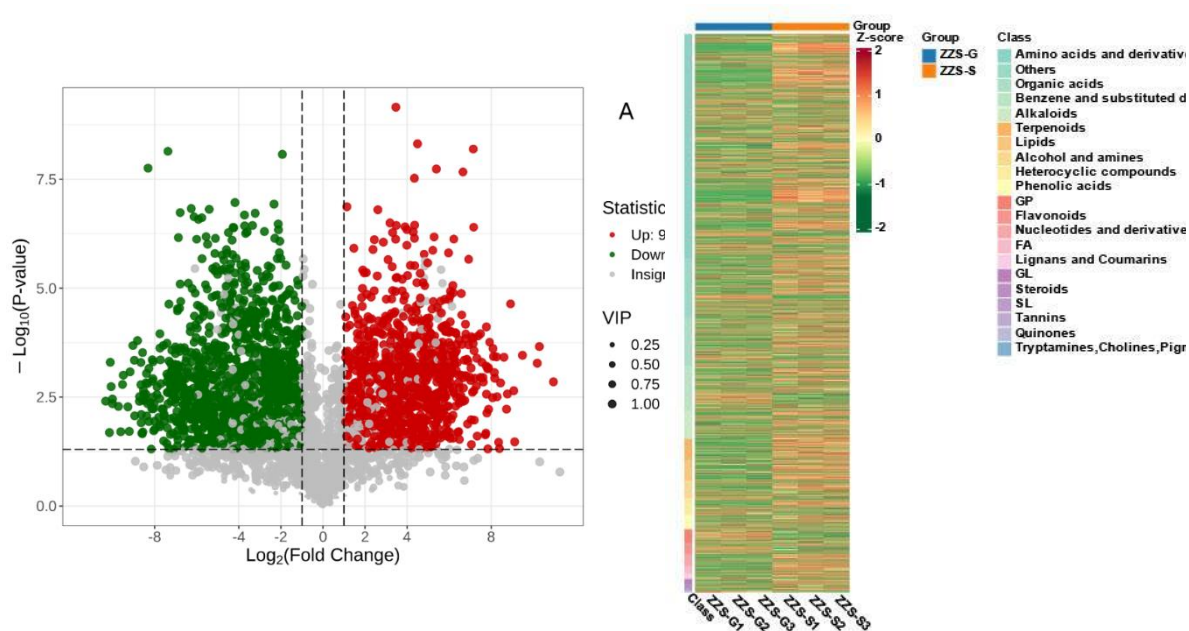


Figure 11. Volcano plot and cluster analysis heatmap. In the volcano plot (A), each point is a metabolite: red for upregulation, green for downregulation, and gray for metabolites present without significant change. Among them. (B) Cluster analysis heatmap.

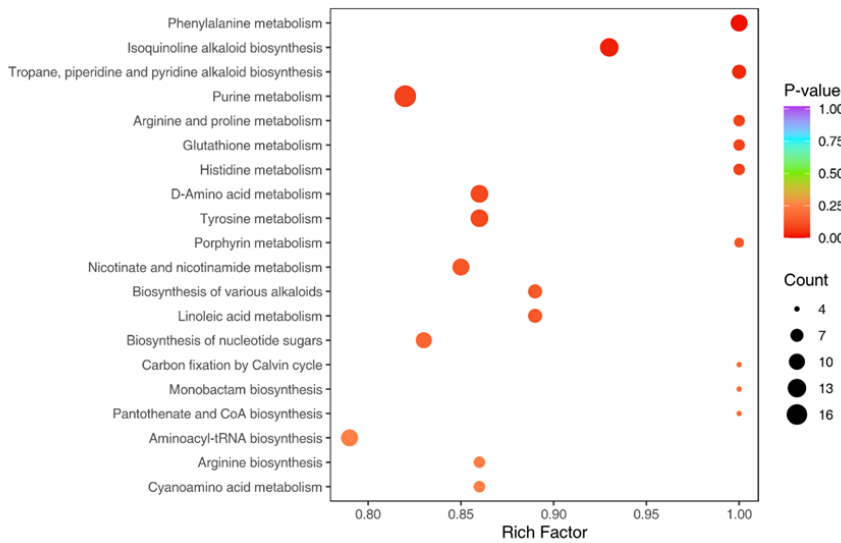


Figure 12. Differential metabolite KEGG enrichment analysis. The Rich Factor is the ratio of the number of differential metabolites in a pathway to the number of annotated metabolites in the pathway. An enrichment greater than one is indicated by a rich factor greater than one.

2.8. MTS Experimental Results Analysis

The result of MTS experimental shows that among the 75% ethanol extract of *Panax japonicus* var. *major* (fresh and dried groups) and chikusetsu saponin IVa inhibited the proliferation of HGC-27 gastric cancer cells. The inhibitory effects of both compounds increased in a dose-dependent manner. The IC_{50} value of the 75% ethanol extract of dried and fresh *Panax japonicus* var. *major* were 104.6 $\mu\text{g/mL}$ and 440.8 $\mu\text{g/mL}$, whereas chikusetsu saponin IVa exhibited an IC_{50} value of 564.7 $\mu\text{g/mL}$. These results confirm that both compounds possess notable anticancer activity against HGC-27 cells. Moreover, the activity of the dry group was significantly higher than the activity of the fresh group.

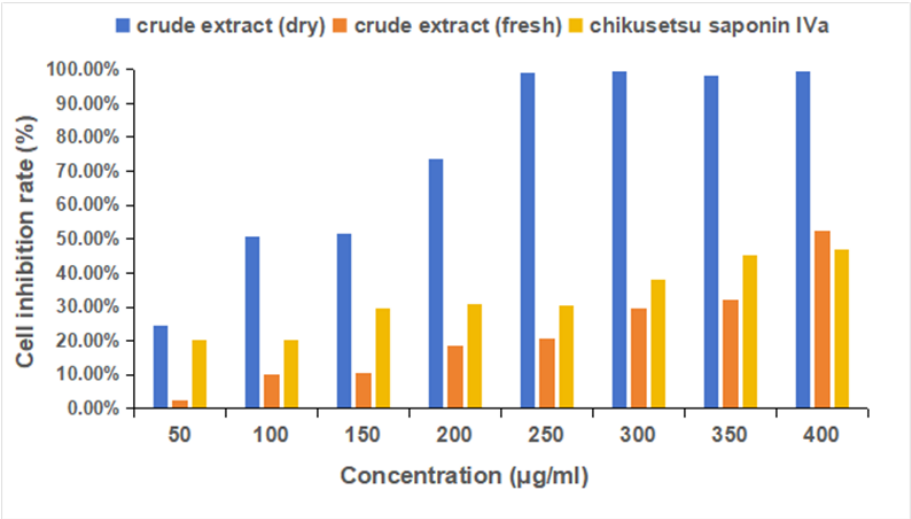
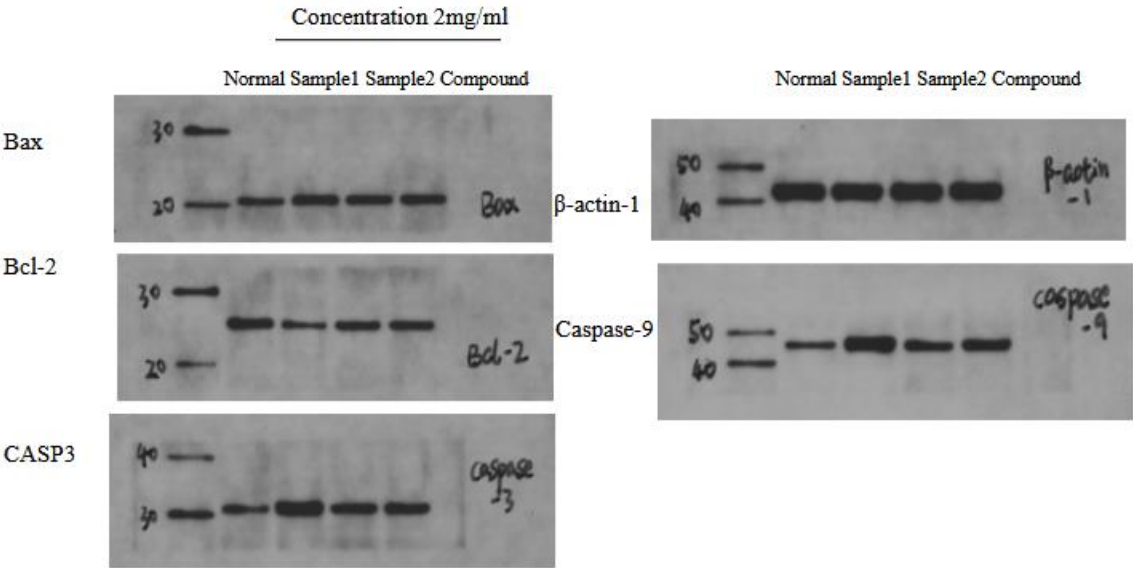


Figure 13. MTS cell (HGC-27) inhibition rate assay, the sample was 75% ethanol extract of *Panax japonicus* var. *major*.

2.9. Western Blot Results Analysis

Figure 14 and 15 indicate that treatment with the 75% ethanol extract of *Panax japonicus* var. *major* and chikusetsu saponin IVa significantly upregulated the expression of CASP3 and Caspase-9 proteins, thereby inducing apoptosis in HGC-27 cells. Additionally, Bax protein expression was markedly increased, while Bcl-2 protein levels were reduced, further enhancing apoptotic processes and inhibiting cell proliferation. The expression of TNF- α protein was notably downregulated, whereas AKT1 and EGFR protein levels were elevated following treatment with the compounds.



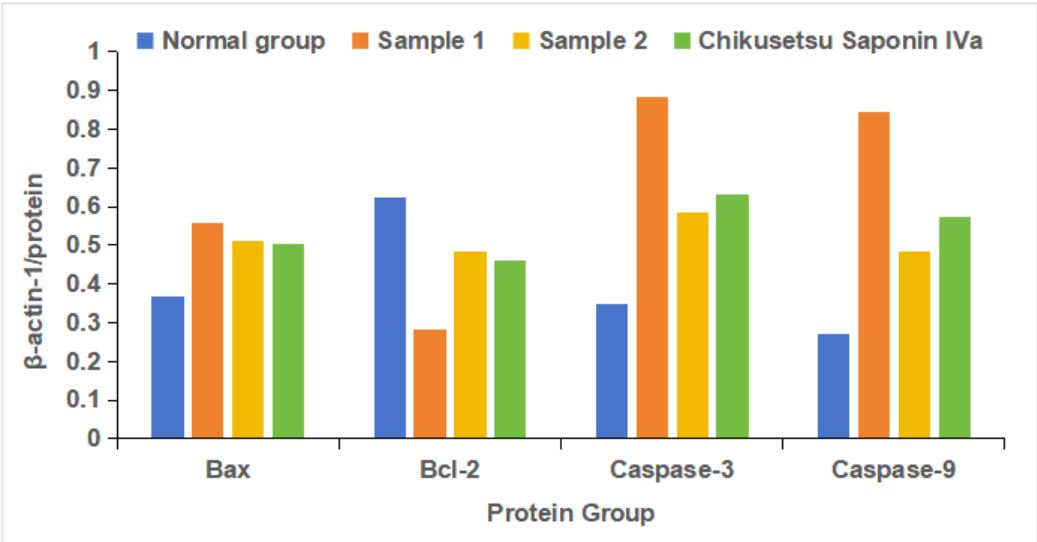


Figure 14. Western blot analysis the treatment groups were administered at a concentration of 2mg/ml, Sample1and Sample 2 were 75% ethanol extract of *Panax japonicus* var. *major*. (Sample1 was dry *Panax japonicus* var. *major*. Sample 2 was fresh *Panax japonicus* var. *major*.).

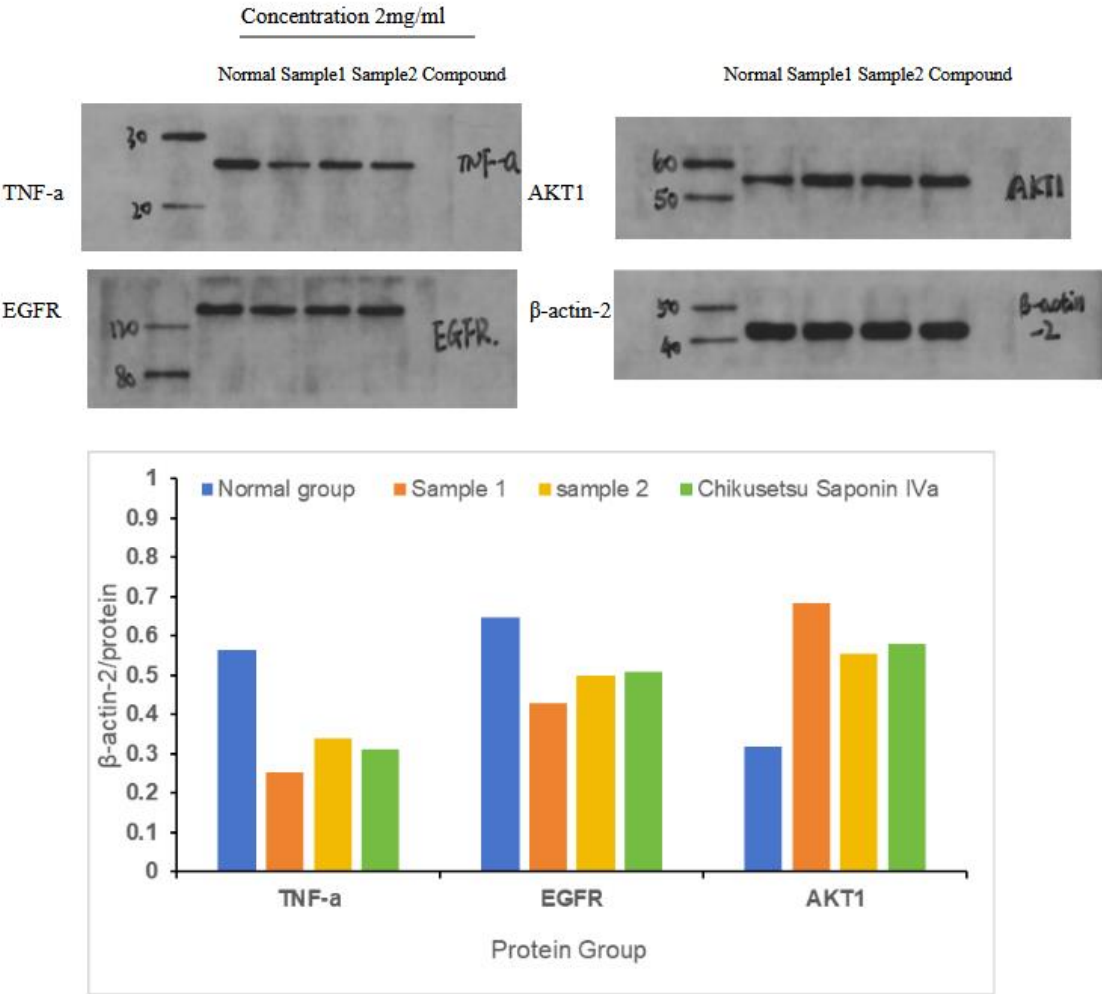


Figure 15. Western blot analysis the treatment groups were administered at a concentration of 2mg/ml, Sample1and Sample 2 were 75% ethanol extract of *Panax japonicus* var. *major*. (Sample1 was dry *Panax japonicus* var. *major*. Sample2 was fresh *Panax japonicus* var. *major*.).

3. Discussion

P. japonicus var. *major*, as a traditional medicinal plant, shows similar physical characteristics and medicinal effects with ginseng, possessing a rich medical material foundation and significant medicinal value. It primarily functions to nourish the lungs and Yin, improve blood circulation, relieve pain, and stop bleeding [35], gaining widespread application in folk medicine of ethnic groups. The Naxi people used *P. japonicus* var. *major* as a daily health supplement, commonly made for soaking in alcohol or cooking in soup to enhance immunity and protect the gastric mucosa [36]. Additionally, *P. japonicus* var. *major* was also applied in treating stomach pain, pharyngitis, and swollen sores. the rhizome of *P. japonicus* var. *major* was used by Bai people to treat modern common diseases such as gastric pain and lymphoma, and for anti-tumor treatment have been recorded in ethnic classic medical books. Pharmacological research found that certain saponin active compounds contained in *P. japonicus* var. *major* possessed anti-cancer and liver-protective effects [21], while its small amounts of flavonoids and triterpene saponin compounds simultaneously exhibited anti-inflammatory and antioxidant properties [23]. Overall, while *P. japonicus* var. *major* has demonstrated anti-tumor efficacy, its underlying mechanisms are complex, involving multiple components and targets.

Network pharmacology is an emerging research methodology that integrates systems biology, bioinformatics, and computer science to construct drug-target-disease networks and reveal the systemic mechanisms of anti-tumor drugs. This approach can analyze the effective components and targets of traditional Chinese medicine formulations, elucidate the molecular mechanisms of their synergistic anti-tumor effects, while identifying key tumor nodes and pathways to provide potential targets for new drug development and accelerate the drug development process.[37–39]

Network pharmacology, we predicted the activity of compounds extracted from *P. japonicus* var. *major* against gastric cancer (GC) and explored the potential molecular mechanisms of their anti-GC properties in this study. First, we assembled a list of chemical compounds present in *P. japonicus* var. *major* extracts, yielding 44 active compounds from the ETCM database, with 355 predicted target proteins based on the Swiss Target Prediction database. We separately curated a list of 2,103 GC targets from the Gene Cards and OMIM databases. Second, we defined 125 common targets shared between targets of *P. japonicus* var. *major* active compounds and GC targets, which we used to construct a protein–protein interaction (PPI) network. The main core targets obtained from the PPI network, including AKT1, TNF, EGFR and CASP3, are directly related to apoptosis and are known to cause inflammation in GC cells. Third, we determined the top 10 GO terms and 20 KEGG pathways enriched among the 29 core targets. The core targets were mainly localized in the cytoplasm and nucleus, where they bind to proteins and enzymes [40,41], and had functions related to protein phosphorylation. We determined that *P. japonicus* var. *major* acts against GC through the TNF and T-cell receptor signaling pathways via the binding of its characteristic saponins to the core targets TNF and CASP3 in those two signaling pathways, which are highly important in cancer and inflammation [42–44]. We found that 3 compounds interacted with CASP3; 1 compound interacted with TNF; 2 compounds interacted with AKT1; 5 compounds interacted with EGFR. EGFR is a transmembrane receptor tyrosine kinase that plays a key role in various cellular biological processes including cell proliferation, differentiation, migration, and survival. EGFR has a close relationship with the occurrence, development, and treatment of cancer [45,46]. AKT1 is a core member of the PI3K/AKT/mTOR signaling pathway and exhibits overactivation or mutations (especially the E17K mutation) in various cancers, promoting tumor development through multiple mechanisms including inhibition of apoptosis, enhancement of cell proliferation, regulation of cellular metabolism, and angiogenesis; its abnormal activation is not only closely associated with tumor progression but also involved in tumor resistance mechanisms to chemotherapy, radiotherapy, and targeted therapies.[47]

According to the result of network pharmacology analysis, we explored the potential mechanisms of the active compounds in *P. japonicus* var. *major* in the treatment of GC based on molecular docking and other predictions. We chose two compounds (Chikusetsu saponin IVa and

calenduloside E) with high values as ligands for molecular docking analysis. Chikusetsu saponin IVa is typically used as a quality standard of traditional Chinese medicine [48]. Both compounds were previously reported to show excellent activity against hepatocellular carcinoma [49]. From a compound–target network, we selected the four targets AKT1, TNF, EGFR, and CASP3 for molecular docking analysis. Six of the eight compound–target pairs (Chikusetsu saponin IVa–AKT1, Chikusetsu saponin IVa–CASP3, Chikusetsu saponin IVa–EGFR, calenduloside E–AKT1, calenduloside E–CASP3, and calenduloside E–EGFR) had strong binding characteristics, with the other two pairs (Chikusetsu saponin IVa–TNF, calenduloside E–TNF) showing weaker but still high binding properties. These molecular docking results align with the findings from our network pharmacological analysis.

To evaluate the result of molecular docking, molecular dynamics simulations and free binding energy calculations for the Chikusetsu saponin IVa–CASP3 complex indicated that the complex is structurally stable, as indicated by the calculated RMSD values. RMSF and SASA calculations for the complex after secondary structure stabilization suggested that the CASP3 surface area becomes smaller following saponin binding. Calculations of H-bonds and binding free energy showed that Chikusetsu saponin IVa forms many H-bonds with CASP3 and has a strong binding capacity. The CASP3–Chikusetsu saponin IVa complex had an energy minimum mainly focused on 99 ns according to the free energy landscape. The complex was relatively compact and structurally stable in this low-energy region.

To investigate the differences in anti-gastric cancer activity between fresh and dried *P. japonicus* var. *major* ethanol extracts, we conducted a non-targeted metabolomics study on the two crude extracts. The research found that between the dried group (ZZG) and fresh group (ZZS) *P. japonicus* var. *major* crude extracts, there were significant changes in the content of 2,301 differential metabolites, among which 914 metabolites were significantly upregulated and 1,297 significantly downregulated. Among the top 20 metabolites with the highest fold changes between the two groups, there are Notoginsenoside J and 2-(3,4-dihydroxy-5-methoxyphenyl)-5,6,7-trihydroxy-3,4-dihydro-2H-1-benzopyran-4-one, a flavonoid compound. These potential active compounds with anti-cancer activity require further experimental verification.

To further validated the effects of the *P. japonicus* var. *major* and active compounds indentified through binding energy predictions, in vitro experiments were implemented. First, the results of the MTS assay demonstrated that among the the 75% ethanol extract of *Panax japonicus* var. *major* (Fresh group and dried group) and chikusetsu saponin IVa effectively suppressed the growth of HGC-27 gastric cancer cells. Moreover, the anti-gastric cancer cell activity of dried *Panax japonicus* crude extract was significantly higher than that of fresh *Panax japonicus* extract. Based on untargeted metabolomics analysis, the significant difference in anti-gastric cancer activity between extracts from fresh and dried samples are likely attributable not only to the varying abundance of metabolites, but also to the involvement of specific metabolic pathways. These pathways include phenylalanine metabolism, isoquinoline alkaloid biosynthesis, tropane, piperidine and pyridine alkaloid biosynthesis, as well as arginine biosynthesis. Changes in the levels of metabolites within these pathways may be closely associated with the observed differences in bioactivity and could have potential implications for the pathophysiology of gastric cancer. Second,western Blot analysis revealed that these compounds promote apoptosis by increasing the expression of CASP3 and Caspase-9 proteins. Furthermore, they modulate the apoptotic regulatory pathway by upregulating Bax and downregulating Bcl-2, thereby enhancing pro-apoptotic activity and inhibiting tumor cell survival. The observed reduction in TNF- α expression suggests that these compounds may also alleviate inflammation, potentially reducing the risk of inflammation-induced gastric cancer. Collectively, these findings suggest that the the 75% ethanol extract of *Panax japonicus* var. *major* and chikusetsu saponin IVa hold promise as therapeutic agents for gastric cancer through their dual roles in promoting apoptosis and modulating inflammatory responses. Finally, these findings suggest that *Panax japonicus* var. *major* regulates the intersected targets and pathways through these core compounds,thereby exerting therapeutic effects on gastric cancer. In summary, the western blot

experiments further validated the prediction made through network and molecular docking, molecular docking, providing molecular evidence that *Panax japonicus* var. *major* had potential anti-cancer effects.

In this study, we systematically explored the mechanisms of *P. japonicus* var. *major* for the treatment of GC. Our predictions of the interaction between the targets of *P. japonicus* var. *major* compounds and GC targets should help provide a theoretical basis for the further development of traditional Chinese medicines. Importantly, clinical trials are needed to further explore the medicinal value of *P. japonicus* var. *major* in cancer. Through network pharmacology, we identified the major active compounds and potential mechanisms of *P. japonicus* var. *major* in anti-gastric cancer activity, and verified its anti-gastric cancer biological activity through experiments. The study found that the significant difference in anti-gastric cancer cell activity between fresh and dried *P. japonicus* var. *major* crude extracts is related to the changes in differential metabolite content and pathway enrichment between the two. However, whether these differential metabolites actually possess anti-gastric cancer biological activity and their specific mechanisms of action still require further experimental verification.

4. Materials and Methods

4.1. Medicinal Materials, Chemicals

Medicinal Herb: *P. japonicus* var. *major* (dried samples and fresh samples) is provided by Xinzhu Village, Ludian Township, Yulong Naxi Autonomous County, Lijiang City, Yunnan Province. It has been identified by Lixin Yang, a senior engineer at the Kunming Institute of Botany, Chinese Academy of Sciences, Yunnan Province. Chikusetsu saponin IVa reference standard (CAS No.: 51415-02-2) was provided by Shanghai Yuanye Co., Ltd., with a purity greater than 98%.

4.2. Collection of Main Active Compounds and Corresponding Targets

The known active compounds of *P. japonicus* var. *major* were obtained from The Encyclopedia of Traditional Chinese Medicine database (<http://www.tcmip.cn/ETCM/>) [50]. The chemical structures for these active compounds were obtained from the PubChem database (<https://pubchem.ncbi.nlm.nih.gov/>). The potential targets of these active compounds were predicted by the Swiss Target Prediction tool (<http://www.swisstargetprediction.ch/>) [51].

4.3. Collection of Disease-Related Targets

Targets for treating GC were obtained from searches at the databases Gene Cards (<https://www.genecards.org/>) [52] and OMIM (<https://www.omim.org/>) [53], using the keyword “gastric cancer”. The two sets of targets were merged and redundant targets were removed to define a set of non-redundant targets. A Venn diagram was used to predict the overlap between *P. japonicus* var. *major* target genes and putative targets for GC treatment. The shared 125 targets were considered common targets for GC treatment by compounds from *P. japonicus* var. *major*.

4.4. Protein–Protein Interaction (PPI) Network Analysis

Cytoscape 3.10.2 software was used to analyze and visualize the network of potential targets [54]. The common targets defined above were submitted as input to the String database (<https://string-db.org>) to a gene-protein interaction network [55]. First, the main active ingredients and their corresponding targets were collected into Network files. Second, the network comprising the common targets and active ingredients was exported into Tape files. Third, the network files and Tape files were imported into Cytoscape3.10.2 to diagram the compound–target network. The Cytoscape3.10.2 filtering conditions were set to closeness > 0.046, betweenness > 99.70, degree > 33.07. The resulting PPI network allowed us to predict the main compounds with potential anti-GC effects and their corresponding core targets.

4.5. Gene Ontology Term Enrichment and Kyoto Encyclopedia of Genes and Genomes Pathway Enrichment Analysis

The gene ontology (GO) term and Kyoto Encyclopedia of Genes and Genomes (KEGG) pathway enrichment analysis was carried out on the 29 core targets through the DAVID database (<https://david.ncicfcrf.gov/>) [56], with the setting “*Homo sapiens*”. The corresponding Biological Process (BP), Cellular Component (CC), Molecular Function (MF) terms, and KEGG pathways were analyzed as indicated above and visualized with the ggplot2, openxls, and tidyverse packages in R. The top 20 KEGG pathways were used to construct a component–target–pathway diagram through cytoscape10.3.2 combined with the main active ingredients and the core targets of GC.

4.6. Survival Analysis

Analysis of the potential effect of inhibiting these targets on survival of GC patients was carried out using the online tool Kaplan-Meier Plotter (<https://kmplot.com/analysis/>) [57]. Disease type was selected as “gastric cancer” and the species was set to “human”. A *P* value < 0.05 was set as threshold for statistical significance. Survival analysis could predict factors affect patient survival time. The potential effects of changes in target protein abundance/activity were analyzed according to whether high or low expression of each gene was beneficial for patient survival.

4.7. Molecular Docking Analysis

Molecular Operating Environment 2019 (MOE2019) and PyMol2.6.0 were used for molecular docking and to visualize the top four core targets and the top two compounds. MOE2019 software was used to estimate the energy minimization of compounds. The Protein Data Bank (PDB, <https://www.rcsb.org/>) [58] was used to download protein structures in the correct format for this analysis. The 3D structures of the active compounds were downloaded from the PubChem database (<https://pubchem.ncbi.nlm.nih.gov/>). The format of these structure files was transformed mol2 format through OPen Babel Gui software. Energy minimization of each compound was performed using MOE2019 software. Finally, molecular docking was conducted by MOE 2019 software with 50 operations. The binding activity was assessed based on the magnitude of binding energy and the results were visualized in PyMOL2.6.0 and Discovery studio 2019 software.

4.8. Molecular Dynamics Simulations and Calculation of Binding Free Energies

Gromacs2022.3 software [59,60] was used for molecular dynamics simulations. For small molecule preprocessing, amberTools22 was used to add the GAFF force field to the small molecules and Gaussian 16W was used to simulate the hydrogenation of small molecules and calculate their RESP potential. The potential data were added to the topology file of the molecular dynamics system. The simulation conditions were a constant temperature of 300K and atmospheric pressure (1 bar). Amber99sb-ildn was used as force field and water molecules were used as solvent (Tip3p water model), and the total charge of the simulation system was neutralized by adding an appropriate number of sodium (Na⁺) ions. The simulation system adopted the steepest descent method to minimize the energy, and then carried out isothermal isovolumic ensemble (NVT) equilibrium and isothermal isobaric ensemble (NPT) equilibrium for 100,000 steps, respectively, with a coupling constant of 0.1 ps and a duration of 100 ps. Finally, free molecular dynamics simulation was performed. The procedure consisted of 5,000,000 steps, with a step length of 2 fs and a total duration of 100 ns. After the simulation was completed, the built-in tool of the software was used to analyze the trajectory, and the root-mean-square variance (RMSD), root-mean-square fluctuation (RMSF), and protein rotation radius of each amino acid trajectory were calculated and combined with the free energy (MMGBSA), free energy topography, and other data.

4.9. Untargeted Metabolomics

In order to compare the differential metabolites and determine the anti-gastric cancer activity between fresh *P. japonicus* var. *major* and its dried, saponin-enriched counterpart, non-targeted metabolomics analysis was conducted with 75% ethanol crude extracts (ZZS-G group is crude extract of dried *P. japonicus* var. *major* and ZZS-S is crude extract of fresh *P. japonicus* var. *major*). Each sample had 600 μL of 70% methanol added to it along with an internal standard solution. The internal standard was prepared by dissolving 1 mg of reference material in 1 mL of 70% methanol to obtain a stock solution (1000 $\mu\text{g/mL}$), which was diluted to a working concentration of 250 $\mu\text{g/mL}$. The solution was centrifuged at 12,000 rpm for 3 minutes, and the supernatant was filtered through a 0.22 μm microporous membrane and transferred to autosampler vials for UPLC-MS/MS analysis. Chromatographic separation was achieved with a Waters ACQUITY UPLC HSS T3 column (1.8 μm , 2.1 mm \times 100 mm). The mobile phase consisted of 0.1% formic acid in ultrapure water (solvent A) and 0.1% formic acid in acetonitrile (solvent B). The column temperature was 40 $^{\circ}\text{C}$, the flow rate was 0.40 mL/min, and the injection volume was 4 μL .

4.10. MTS Cell Inhibition Rate

A single-cell suspension was prepared using RPMI 1640 culture medium supplemented with 10% fetal bovine serum (FBS). A total of 5000 cells were seeded into each well of a 96-well plate, with a final volume of 100 μL per well. The cells were incubated for 12–24 hours to allow for adherence prior to treatment. The test sample1 and sample2 (the 75% ethanol extract of *Panax japonicus* var. *major* (dry group and fresh group) and chikusetsu saponin IVa compound (Purchased from Shanghai Yuanye company) were dissolved in DMSO and initially screened at concentrations of 400 $\mu\text{g/mL}$, 350 $\mu\text{g/mL}$, 300 $\mu\text{g/mL}$, 250 $\mu\text{g/mL}$, 200 $\mu\text{g/mL}$, 150 $\mu\text{g/mL}$, 100 $\mu\text{g/mL}$, and 50 $\mu\text{g/mL}$. A final volume of 200 μL , containing the compound, was added to each well. Each treatment was performed in triplicate. Following 48 hours of incubation at 37 $^{\circ}\text{C}$, 20 μL of MTS solution and 100 μL of culture medium were added to each well. Blank control wells were included, and the cells were incubated for an additional 2–4 hours to ensure complete reaction. The absorbance was subsequently measured at 492 nm using a microplate reader. Doxorubicin (Dox) and paclitaxel (Taxol) were used as positive controls.

4.11. Western Blotting

HGC-27 cells were seeded at a density of 2×10^5 cells/mL in 6-well plates and incubated for 24 hours, the drug concentration was 2 mg/mL. After incubation, the cells were divided into treatment groups and cultured for an additional 24 hours. Subsequently, the cells were washed twice with ice-cold PBS, and total protein was extracted using RIPA lysis buffer. Following denaturation, 20 μL of the protein samples were loaded into each well of an SDS-PAGE gel for electrophoresis. Proteins were transferred onto a PVDF membrane, which was then blocked with blocking buffer at room temperature for 2 hours under gentle agitation. The membrane was incubated with primary antibodies overnight at 4 $^{\circ}\text{C}$, followed by a 2-hour incubation with secondary antibodies at room temperature. After washing with PBST, the membrane was developed using enhanced chemiluminescence (ECL). The membrane was air-dried, and the resultant images were scanned. Protein bands were quantified based on grayscale intensity using Image-Pro Plus (IPP) software.

5. Conclusions

In this study, we used network pharmacology to screen the main active compounds of *P. japonicus* var. *major* and their potential targets in relation to the treatment of gastric cancer. A protein–protein interaction network allowed us to explore the interaction between the main compounds of *P. japonicus* var. *major* and their putative targets related to GC, as well as their potential mechanisms of action against GC. Predictions from network pharmacology suggest that Chikusetsu saponin IVa and calendulose E have good anti-GC activity, and this was supported by survival analysis, molecular docking, combined with molecular dynamics simulations and binding free energy calculations. We

assessed the structural stability, energy nadir, and change in binding energy of drug small molecules bound to four target proteins, the anti-gastric cancer activity and mechanism of 75% ethanol crude extract and chikusetsu saponin IVa compound were verified through MTS cell inhibition assay and Western Blot analysis. Meanwhile, through the application of untargeted metabolomics, the differential metabolic products of pearl ginseng were analyzed to explore the factors contributing to the differences in anti-gastric cancer activity between fresh and dried groups. We carried out a comprehensive analysis of the binding possibilities and accuracy of the molecules revealed by the simulations, which provided possibilities for potential anti-GC effects and mechanisms of action for Chikusetsu saponin IVa of *P. japonicus* var. *major*.

Declaration of competing interests: The authors declared no conflict of interest between author and publication.

Authors’ contributions: **Chao Huang:** Data collection, Formal analysis, Methodology, Resources, Visualization, Writing—original draft, Writing—review & editing. **Xiuxiang Yan:** Data collection, Supervision, Writing—original draft, Writing—review & editing. **Ge Li:** Resources, Supervision, Writing—review & editing. **Terd Disayathanoowat:** Resources, Supervision, Writing—review & editing. **Angkhana Inta:** Resources, Writing—review & editing. **Lu Gao:** Resources, Writing—review & editing. **Lixin Yang:** Supervision, Funding acquisition, Writing—review & editing.

Funding information: This work was funded by Lijiang Yunxin Green Biological Development Co., Ltd. (No. E2524812C1), the National Nature Science Foundation of China (31970357), a Trans-boundary cooperation on biodiversity research and conservation in the Gaoligong Mountains (No. E1ZK251), the Yunnan International Joint Laboratory of Southeast Asia Biodiversity Conservation, Menglun, Yunnan, 666303, China, and a grant from the Yunnan Province Science and Technology Department, No. 202203AP140007. Southeast Asia Biodiversity Research Institute, Chinese Academy of Sciences (Grant Nos. 2015CASE-ABRIRG001).

Acknowledgments: This research work was partially supported by Chiang Mai University.

Abbreviations

Full name	Abbreviation
Gastric cancer	GC
Encyclopedia of Traditional Chinese Medicine	ETCM
Kyoto Encyclopedia of Genes and Genomes	KEGG
Gene Ontology	GO
Molecular Dynamics	MD
Root-Mean-Square Deviation	RMSD
Root Mean Square Fluctuation	RMSF
Molecular Mechanics Poisson-Boltzmann Surface Area	MMPBS
Fetal Bovine Serum	FBS
Enhanced Chemiluminescence	ECL
Image-Pro Plus	IPP
Dried <i>P. japonicus</i> var. <i>major</i> Group	ZZS-G
Fresh <i>P. japonicus</i> var. <i>major</i> Group	ZZS-S

References

1. F. Bray, M. Laversanne, H. Sung, J. Ferlay, R.L. Siegel, I. Soerjomataram, A. Jemal, Global cancer statistics 2022: GLOBOCAN estimates of incidence and mortality worldwide for 36 cancers in 185 countries, *CA: A Cancer Journal for Clinicians*. 2024, 74, 229-263. <https://doi.org/10.3322/caac.21834>
2. J.A. Ajani, T.A. D’Amico, D.J. Bentrem, J. Chao, D. Cooke, C. Corvera, P. Das, P.C. Enzinger, T. Enzler, P. Fanta, F. Farjah, H. Gerdes, M.K. Gibson, S. Hochwald, W.L. Hofstetter, D.H. Ilson, R.N. Keswani, S. Kim, L.R. Kleinberg, S.J. Klempner, J. Lacy, Q.P. Ly, K.A. Matkowskyj, M. McNamara, M.F. Mulcahy, D. Outlaw, H. Park, K.A. Perry, J. Pimiento, G.A. Poultsides, S. Reznik, R.E. Roses, V.E. Strong, S. Su, H.L. Wang, G. Wiesner, C.G. Willett, D. Yakoub, H. Yoon, N. McMillian, L.A. Pluchino, Gastric Cancer, Version 2.2022, NCCN Clinical Practice Guidelines in Oncology, *Journal of the National Comprehensive Cancer Network*. 2022,20, 167-192. <https://doi.org/10.6004/jnccn.2022.0008>
3. S. Vijayalakshmi, D.-S. Yoo, D.-G. Kim, R. Chelliah, K. Barathikannan, S.-O. Aloo, A. Tyagi, P. Yan, L. Shan, T.S. Gebre, D.-H. Oh, Fermented *Perilla frutescens* leaves and their untargeted metabolomics by UHPLC-

- QTOF-MS reveal anticancer and immunomodulatory effects, *Food Bioscience*. 2023, 56. <https://doi.org/10.1016/j.fbio.2023.103065>
4. Z. Wang, R. Wang, Z. Na, S. Liang, F. Wu, H. Xie, X. Zhang, W. Xu, X. Wang, Network Pharmacology Analysis of Liquid-Cultured *Armillaria ostoyae* Mycelial Metabolites and Their Molecular Mechanism of Action against Gastric Cancer, *Molecules*. 2024, 29. <https://doi.org/10.3390/molecules29071668>
 5. K. Gao, W. Cao, Z. He, L. Liu, J. Guo, L. Dong, J. Song, Y. Wu, Y. Zhao, Network medicine analysis for dissecting the therapeutic mechanism of consensus TCM formulae in treating hepatocellular carcinoma with different TCM syndromes, *Frontiers in Endocrinology*. 2024, 15. <https://doi.org/10.3389/fendo.2024.1373054>
 6. D. Lu, L. Yuan, X. Ma, F. Meng, D. Xu, S. Jia, Z. Wang, Y. Li, Z. Zhang, Y. Nan, The mechanism of polyphyllin in the treatment of gastric cancer was verified based on network pharmacology and experimental validation, *Heliyon*. 2024, 10. <https://doi.org/10.1016/j.heliyon.2024.e31452>
 7. Y. Ji, Y. Liu, J. Hu, C. Cheng, J. Xing, L. Zhu, H. Shen, S.M. Silvestre, Exploring the Molecular Mechanism of *Astragali Radix-Curcumae Rhizoma* against Gastric Intraepithelial Neoplasia by Network Pharmacology and Molecular Docking, *Evidence-Based Complementary and Alternative Medicine*. 2021, 1-11. <https://doi.org/10.1155/2021/8578615>
 8. Y. Wei, X. Yu, J. Tang, L. Yin, Z. Wu, J. Zhang, Y. Gao, Analysis of Network Pharmacology and Molecular Docking on *Radix Pseudostellariae* for Its Active Components on Gastric Cancer, *Applied Biochemistry and Biotechnology*. 2022, 195,1968-1982. <https://doi.org/10.1007/s12010-022-04263-2>
 9. V. Zoi, V. Galani, G.D. Lianos, S. Voulgaris, A.P. Kyritsis, G.A. Alexiou, The Role of Curcumin in Cancer Treatment, *Biomedicines*. 2021, 9. <https://doi.org/10.3390/biomedicines9091086>
 10. A. Duda-Madej, S. Viscardi, W. Szewczyk, E. Topola, Natural Alkaloids in Cancer Therapy: Berberine, Sanguinarine and Chelerythrine against Colorectal and Gastric Cancer, *International Journal of Molecular Sciences*. 2024, 25. <https://doi.org/10.3390/ijms25158375>
 11. Y.-w. Sun, Y. Ju, C.-h. Liu, K.-c. Du, D.-l. Meng, Polyhydroxyl guaianolide terpenoids as potential NF- κ B inhibitors induced cytotoxicity in human gastric adenocarcinoma cell line, *Bioorganic Chemistry*. 2020, 95. <https://doi.org/10.1016/j.bioorg.2019.103551>
 12. A. Rauf, P. Wilairatana, P.B. Joshi, Z. Ahmad, A. Olatunde, N. Hafeez, H.A. Hemeg, M.S. Mubarak, Revisiting luteolin: An updated review on its anticancer potential, *Heliyon*. 2024, 10. <https://doi.org/10.1016/j.heliyon.2024.e26701>
 13. X. Liu, K. Sun, X. Jin, X. Wu, M. Xia, Y. Sun, L. Feng, G. Li, X. Wan, C. Chen, Review on active components and mechanism of natural product polysaccharides against gastric carcinoma, *Heliyon*. 2024, 10. <https://doi.org/10.1016/j.heliyon.2024.e27218>
 14. S. Duan, J. Yin, Z. Bai, Z. Zhang, Effects of taxol resistance gene 1 on the cisplatin response in gastric cancer, *Oncology Letters*. 2018. <https://doi.org/10.3892/ol.2018.8390>
 15. J.-Z. Liu, J. Liu, D.-X. Wang, Q. Luo, Z. Liu, Activity tracking isolation of *Gelsemium elegans* alkaloids and evaluation of their antihuman gastric cancer activity in vivo, *Chinese Journal of Analytical Chemistry*. 2021, 49, 91-102. <https://doi.org/10.1016/j.cjac.2021.10.007>
 16. S. Ma, Y. Hu, J. Chen, X. Wang, C. Zhang, Q. Liu, G. Cai, H. Wang, J. Zheng, Q. Wang, L. Zhong, B. Yang, S. Zhou, Y. Liu, F. Han, J. Wang, J. Wang, Marine fungus-derived alkaloid inhibits the growth and metastasis of gastric cancer via targeting mTORC1 signaling pathway, *Chemico-Biological Interactions*. 2023, 382. <https://doi.org/10.1016/j.cbi.2023.110618>
 17. Li, H.Y., Wang, H.Y., Na, L.S., Jin, C.H., Wang, J.L. Ideal solution ranking based on principal component analysis, orthogonal partial least squares discriminant analysis and weighted approximation-gray Evaluating the quality of bead ginseng from different origins by correlation fusion modeling. *Chinese Traditional and Herbal Drugs*. 2024. DOI:10.7501/j.issn.0253-2670.2024.09.025
 18. D. Zhang, L. Dan, T. Gao, Y. Zhang, C. Gong, C. Liu, Y. Li, X. Song, *Panax majoris* Rhizoma: A Comprehensive Review of Phytochemistry, Pharmacology and Clinical Applications, *Records of Natural Products*. 2024, 53-94. <http://dx.doi.org/10.25135/rnp.425.2310.2917>

19. X. Guo, J. Ji, J. Zhang, X. Hou, X. Fu, Y. Luo, Z. Mei, Z. Feng, Anti-inflammatory and osteoprotective effects of Chikusetsusaponin IVa on rheumatoid arthritis via the JAK/STAT signaling pathway, *Phytomedicine*. 2021, 93. <https://doi.org/10.1016/j.phymed.2021.153801>
20. M. Li, X. Li, L. Zhou, Y. Jin, Effects of total saponins from *Panacis majoris* Rhizoma and its degradation products on myocardial ischemia-reperfusion injury in rats, *Biomedicine & Pharmacotherapy*. 2020, 130. <https://doi.org/10.1016/j.biopha.2020.110538>
21. T. Zuo, Z. Zhang, P. Jiang, R. Zhang, D. Ni, Y. Yuan, S. Zhang, Characterization of chikusetsusaponin IV and V induced apoptosis in HepG2 cancer cells, *Molecular Biology Reports*. 2022, 49, 4247-4255. <https://doi.org/10.1007/s11033-022-07259-7>
22. L. Chang, R. Zhou, Y. He, M. Meng, J. Hu, Y. Liu, Y. Pan, Z. Tang, Z. Yue, Total saponins from Rhizoma *Panacis Majoris* inhibit proliferation, induce cell cycle arrest and apoptosis and influence MAPK signalling pathways on the colorectal cancer cell, *Molecular Medicine Reports*. 2021, 24. <https://doi.org/10.3892/mmr.2021.12181>
23. M.-H. Chen, D.-J. Li, H.-B. He, X.-M. Li, Y.-H. Ding, Y.-F. Zhang, H.-Y. Xu, M.-L. Feng, C.-Q. Xiang, J.-G. Zhou, J.-H. Zhang, H.-J. Liu, Saponins from Rhizoma *Panacis Majoris* attenuate myocardial ischemia/reperfusion injury via the activation of the Sirt1/Foxo1/Pgc-1 α and Nrf2/antioxidant defense pathways in rats, *Pharmacognosy Magazine*. 2018, 14. http://dx.doi.org/10.4103/pm.pm_467_17
24. Zhang, M.X., Fang, F., Yang, Y., Fan, J.L., Yuan, P. Protective effect of ginsenoside Rg1 on hypoxic-ischemic brain injury and neuronal apoptosis in young rats. *Journal of Xi an Jiaotong University*. 2021. 10.7652/jdyxb202105009
25. Z. Ai, S. Liu, J. Zhang, Y. Hu, P. Tang, L. Cui, X. Wang, H. Zou, X. Li, J. Liu, B. Nan, Y. Wang, Ginseng Glucosyl Oleanolate from Ginsenoside Ro, Exhibited Anti-Liver Cancer Activities via MAPKs and Gut Microbiota In Vitro/Vivo, *Journal of Agricultural and Food Chemistry*, 2024, 72,7845-7860. <https://doi.org/10.1021/acs.jafc.3c08150>
26. X. Tang, M. Zhu, Z. Zhu, W. Tang, H. Zhang, Y. Chen, F. Liu, Y. Zhang, Ginsenoside Re inhibits non-small cell lung cancer progression by suppressing macrophage M2 polarization induced by AMPK α 1/STING positive feedback loop, *Phytotherapy Research*. 2024, 38, 5088-5106. <https://doi.org/10.1021/acs.jafc.3c08150>
27. H.S. Mansour, H.A.A. Abd El-wahab, A.M. Ali, T. Aboul-Fadl, Inversion kinetics of some E/Z 3-(benzylidene)-2-oxo-indoline derivatives and their in silico CDK2 docking studies, *RSC Advances*. 2021, 11, 7839-7850.
28. K. Sargsyan, C. Grauffel, C. Lim, How Molecular Size Impacts RMSD Applications in Molecular Dynamics Simulations, *Journal of Chemical Theory and Computation*. 2017, 13, 1518-1524. <https://doi.org/10.1021/acs.jctc.7b00028>
29. E. Wang, H. Sun, J. Wang, Z. Wang, H. Liu, J.Z.H. Zhang, T. Hou, End-Point Binding Free Energy Calculation with MM/PBSA and MM/GBSA: Strategies and Applications in Drug Design, *Chemical Reviews*. 2019, 119, 9478-9508. <https://doi.org/10.1021/acs.chemrev.9b00055>
30. G. Sharma, R. Shukla, T.R. Singh, Identification of small molecules against the NMDAR: an insight from virtual screening, density functional theory, free energy landscape and molecular dynamics simulation-based findings, *Network Modeling Analysis in Health Informatics and Bioinformatics*. 2022, 11. <https://doi.org/10.1007/s13721-022-00374-2>
31. T. Wiggins, S. Kumar, S.R. Markar, S. Antonowicz, G.B. Hanna, Tyrosine, Phenylalanine, and Tryptophan in Gastroesophageal Malignancy: A Systematic Review, *Cancer Epidemiology, Biomarkers & Prevention*. 2015, 24, 32-38. <https://doi.org/10.1158/1055-9965.epi-14-0980>
32. T. Luo, Z. Li, X.-M. Deng, K. Jiang, D. Liu, H.-H. Zhang, T. Shi, L.-Y. Liu, H.-X. Wen, Q.-E. Li, Z. Wang, Isolation, synthesis and bioactivity evaluation of isoquinoline alkaloids from *Corydalis hendersonii* Hemsl. against gastric cancer in vitro and in vivo, *Bioorganic & Medicinal Chemistry*. 2022, 60. <https://doi.org/10.1016/j.bmc.2022.116705>
33. P. Mochalski, M. Leja, D. Ślefarska-Wolak, L. Mezmale, V. Patsko, C. Ager, A. Królicka, C.A. Mayhew, G. Shani, H. Haick, Identification of Key Volatile Organic Compounds Released by Gastric Tissues as Potential Non-Invasive Biomarkers for Gastric Cancer, *Diagnostics*. 2023, 13. <https://www.mdpi.com/2075-4418/13/3/335#>

34. I. Bednarz-Misa, M.G. Fleszar, P. Fortuna, Ł. Lewandowski, M. Mierzchała-Pasierb, D. Diakowska, M. Krzystek-Korpacka, Altered L-Arginine Metabolic Pathways in Gastric Cancer: Potential Therapeutic Targets and Biomarkers, *Biomolecules*. 2021, 11. <https://www.mdpi.com/2218-273X/11/8/1086#>
35. Zhang W, Liu C, Guo J, et al. Recent advances in research on non-medicinal parts of *Panax Japonici Rhizoma* and *Panax japonicus* var. *major*, *Chinese Journal of Traditional Chinese Medicine*. 2025.
36. Zhang ZQ, Cao L, Song L, et al. Historical evolution and application prospects of *Panax japonicus* var. *major* like medicinal herbs, *Yunnan Journal of Traditional Chinese Medicine and Materia Medica*. 2012, 33(09), 68-71.
37. X. Yan, A. Inta, X. Yang, H. Pandith, T. Disayathanooowat, L. Yang, An Investigation of the Effect of the Traditional Naxi Herbal Formula Against Liver Cancer Through Network Pharmacology, Molecular Docking, and In Vitro Experiments, *Pharmaceutics*. 2024, 17. <https://doi.org/10.3390/ph17111429>
38. S. Qi, X. Liang, Z. Wang, H. Jin, L. Zou, J. Yang, Potential Mechanism of Tibetan Medicine Liuwei Muxiang Pills against Colorectal Cancer: Network Pharmacology and Bioinformatics Analyses, *Pharmaceutics*. 2024, 17.
39. D. Men, J. Dai, Y. Yuan, H. Jiang, X. Wang, Y. Wang, L. Tao, J. Sheng, Y. Tian, Exploration of anti-osteoporotic peptides from *Moringa oleifera* leaf proteins by network pharmacology, molecular docking, molecular dynamics and cellular assay analyses, *Journal of Functional Foods*. 2024, 116. <https://doi.org/10.1016/j.jff.2024.106144>
40. A.J. Siddiqui, S. Elkahoui, A.M. Alshammari, M. Patel, A.E.M. Ghoniem, R.A.H. Abdalla, H. Dwivedi-Agnihotri, R. Badraoui, M. Adnan, Mechanistic Insights into the Anticancer Potential of *Asparagus racemosus* Willd. Against Triple-Negative Breast Cancer: A Network Pharmacology and Experimental Validation Study, *Pharmaceutics*. 2025, 18. <https://doi.org/10.3390/ph18030433>
41. F. Yu, L. Zhao, S. Chu, TCHH as a Novel Prognostic Biomarker for Patients with Gastric Cancer by Bioinformatics Analysis, *Clinical and Experimental Gastroenterology*. 2024, 17, 61-74. <https://doi.org/10.2147/ceg.s451676>
42. E. Van Quickenberghe, D. De Sutter, G. van Loo, S. Eyckerman, K. Gevaert, A protein-protein interaction map of the TNF-induced NF- κ B signal transduction pathway, *Scientific Data*. 2018, 5. <https://doi.org/10.1038/sdata.2018.289>
43. Z. Zhou, S. Xu, L. Jiang, Z. Tan, J. Wang, A Systematic Pan-Cancer Analysis of CASP3 as a Potential Target for Immunotherapy, *Frontiers in Molecular Biosciences*. 2022, 9. <https://doi.org/10.3389/fmolb.2022.776808>
44. T. Shimoi, J. Hashimoto, K. Sudo, A. Shimomura, E. Noguchi, C. Shimizu, M. Yunokawa, K. Yonemori, H. Yoshida, M. Yoshida, T. Kato, T. Kinoshita, T. Fukuda, Y. Fujiwara, K. Tamura, Hotspot mutation profiles of AKT1 in Asian women with breast and endometrial cancers, *BMC Cancer*, 2021, 21. <https://doi.org/10.1186/s12885-021-08869-3>
45. T. Kondo, O. Kikuchi, Y. Yamamoto, T. Sunami, Y. Wang, K. Fukuyama, T. Saito, H. Nakahara, S. Minamiguchi, M. Kanai, A. Sueyoshi, M. Muto, Colorectal cancer harboring EGFR kinase domain duplication response to EGFR tyrosine kinase inhibitors, *The Oncologist*. 2025, 30. <https://doi.org/10.1093/oncolo/oyae113>
46. X. Li, Z. Wu, L. Yuan, X. Chen, H. Huang, F. Cheng, W. Shen, Hesperidin inhibits colon cancer progression by downregulating SLC5A1 to suppress EGFR phosphorylation, *Journal of Cancer*. 2025, 16, 876-887. <https://doi.org/10.7150/jca.104867>
47. J. Wang, W. Chen, Q. Li, R. Yang, X. Lin, P. Han, X. Huang, H. Hu, M.L. Luo, AKT1E17K-Interacting lncRNA SVIL-AS1 Promotes AKT1 Oncogenic Functions by Preferentially Blocking AKT1E17K Dephosphorylation, *Advanced Science*. 2025. <https://doi.org/10.1002/advs.202500919>
48. National Pharmacopoeia Committee. *Pharmacopoeia of the People's Republic of China (I)*; China Pharmaceutical Science and Technology Press: Beijing, China, 2020.
49. S. Wang, X. Chen, J. Cheng, T. Cai, X. Wu, Z. Cheng, S. Qi, Z. Qi, Calunduloside E inhibits HepG2 cell proliferation and migration via p38/JNK-HMGB1 signalling axis, *Journal of Pharmacological Sciences*. 2021, 147, 18-26. <https://doi.org/10.1016/j.jphs.2021.05.005>
50. Y. Zhang, X. Li, Y. Shi, T. Chen, Z. Xu, P. Wang, M. Yu, W. Chen, B. Li, Z. Jing, H. Jiang, L. Fu, W. Gao, Y. Jiang, X. Du, Z. Gong, W. Zhu, H. Yang, H. Xu, ETCM v2.0: An update with comprehensive resource and

- rich annotations for traditional Chinese medicine, *Acta Pharmaceutica Sinica B*. 2023, 13, 2559-2571. <https://doi.org/10.1016/j.apsb.2023.03.012>
51. D. Gfeller, A. Grosdidier, M. Wirth, A. Daina, O. Michielin, V. Zoete, SwissTargetPrediction: a web server for target prediction of bioactive small molecules, *Nucleic Acids Research*. 2014, 42 W32-W38. <https://doi.org/10.1093/nar/gku293>
 52. M. Safran, I. Dalah, J. Alexander, N. Rosen, T. Iny Stein, M. Shmoish, N. Nativ, I. Bahir, T. Doniger, H. Krug, A. Sirota-Madi, T. Olender, Y. Golan, G. Stelzer, A. Harel, D. Lancet, GeneCards Version 3: the human gene integrator, *Database*. 2010, baq020-baq020. <https://doi.org/10.1093/database/baq020>
 53. A. Hamosh, Online Mendelian Inheritance in Man (OMIM), a knowledgebase of human genes and genetic disorders, *Nucleic Acids Research*. 2004, 32, D514-D517. <https://doi.org/10.1093/nar/gki033>
 54. D. Otasek, J.H. Morris, J. Bouças, A.R. Pico, B. Demchak, Cytoscape Automation: empowering workflow-based network analysis, *Genome Biology*. 2019, 20. <https://doi.org/10.1186/s13059-019-1758-4>
 55. T. Tambouratzis, An artificial neural network based approach for online string matching/filtering of large databases, *International Journal of Intelligent Systems*. 2010, 25, 365-385. <https://doi.org/10.1002/int.20412>
 56. B.T. Sherman, M. Hao, J. Qiu, X. Jiao, M.W. Baseler, H.C. Lane, T. Imamichi, W. Chang, DAVID: a web server for functional enrichment analysis and functional annotation of gene lists (2021 update), *Nucleic Acids Research*. 2022, 50, W216-W221. <https://doi.org/10.1093/nar/gkac194>
 57. Q. Su, Q. Lv, R. Wu, Mining expression and prognosis of FOLR1 in ovarian cancer by using Oncomine and Kaplan-Meier plotter, *Pteridines*. 2019, 30, 158-164. <https://doi.org/10.1515/pteridines-2019-0020>
 58. Wang, R., Fang, X., Lu, Y. and Wang, S. The PDB bind database: collection of binding affinities for protein-ligand complexes with known three-dimensional structures. *J Med Chem*, 47. 2004, 2977-2980. <https://doi.org/10.1021/jm030580l>
 59. D. Van Der Spoel, E. Lindahl, B. Hess, G. Groenhof, A.E. Mark, H.J.C. Berendsen, GROMACS: Fast, flexible, and free, *Journal of Computational Chemistry*. 2005, 26, 1701-1718. <https://doi.org/10.1002/jcc.20291>
 60. M.J. Abraham, T. Murtola, R. Schulz, S. Páll, J.C. Smith, B. Hess, E. Lindahl, GROMACS: High performance molecular simulations through multi-level parallelism from laptops to supercomputers, *SoftwareX*. 2015, 1-2, 19-25. <https://doi.org/10.1016/j.softx.2015.06.001>

Disclaimer/Publisher's Note: The statements, opinions and data contained in all publications are solely those of the individual author(s) and contributor(s) and not of MDPI and/or the editor(s). MDPI and/or the editor(s) disclaim responsibility for any injury to people or property resulting from any ideas, methods, instructions or products referred to in the content.